Bioorganic Chemistry 91 (2019) 103115

Contents lists available at ScienceDirect

Bioorganic Chemistry

journal homepage: www.elsevier.com/locate/bioorg

Design, synthesis, molecular modeling and anti-hyperglycemic evaluation of phthalimide-sulfonylurea hybrids as PPARγ and SUR agonists

Mohamed Ayman El-Zahabi[a,*], Eman R. Elbendary[b], Faida H. Bamanie[c], Mohamed F. Radwan[d], Salah A. Ghareib[e], Ibrahim H. Eissa[a,*]

[a] Medicinal Chemistry Department, Faculty of Pharmacy (Boys), Al-Azhar University, Cairo 11884, Egypt
[b] Medicinal Chemistry Department, Faculty of Pharmacy, Mansoura University, Mansoura 35516, Egypt
[c] Biochemistry Department, Faculty of Medicine, King Abdulaziz University, Jeddah 21589, Saudi Arabia
[d] Department of Pharmaceutical Chemistry, Faculty of Pharmacy, King Abdulaziz University, Jeddah 21589, Saudi Arabia
[e] Pharmacology Department, Faculty of Pharmacy, King Abdulaziz University, Jeddah 21589, Saudi Arabia

ARTICLE INFO

Keywords:
Phthalimide
Anti-diabetic
Sulfonylurea
Docking
Pharmacophore
QSAR
ADMET

ABSTRACT

New series of phthalimide-sulfonylurea hybrids were prepared and examined for their *in vivo* anti-hyperglycemic activities in STZ-induced hyperglycemic rats using glibenclamide as a reference drug. Compounds **6c**, **6d**, **6g**, **6h**, **6j** and **6k** induced significant reduction in the blood glucose levels of diabetic rats ranging from 24.43 to 21.43%. Moreover, molecular docking and pharmacophore approaches were carried out to examine binding modes and fit values of the prepared compounds against PPARγ and SUR, respectively. Compounds **6c**, **6d**, **6j** and **6m** exhibited the highest binding free energies against PPARγ. Compounds **6c**, **6j**, **6k**, **6l**, and **6n** showed the highest fit values against the generated pharmacophore model. Also, QSAR technique was carried out to estimate the proposed PPARγ binding affinities and insulin-secreting abilities. The synthesized compounds showed promising estimated activities. *In-silico* ADMET studies were performed to investigate pharmacokinetics of the synthesized compounds. They showed considerable human intestinal absorption with low BBB penetration.

1. Introduction

Type 2 diabetes affects approximately 200 million people worldwide, including more than a quarter of elderly living in developed countries. Diet and exercise are first line treatments along with oral hypoglycemic drugs to achieve the goal of improving glycemic control and preventing both microvascular and macrovascular complications [1,2]. Sulfonylurea receptors (SUR) and peroxisome proliferator-activated gamma receptors (PPARγ) are the main molecular drug targets (receptors) involved in the treatment of type-2 diabetes mellitus [3,4].

Sulfonylureas were the mainstay of anti-diabetic therapy. The second generation sulfonylureas (glipizide **I** and glibenclamide **II**) are widely employed worldwide [5]. These drugs exert their anti-diabetic effect by stimulating insulin secretion from the pancreatic β-cells [6–8]. The sulfonylureas bind with high affinity to the sulfonylurea receptor (SUR), block ATP-sensitive K+ (KATP) channels in the β-cells, and stimulate insulin secretion at both low and high glucose concentration [9,10]. This glucose independent insulinotropic effect of sulfonylurea often leads to hypoglycemia [11,12]. Therefore, agents which induce insulin secretion augmented by desired glucose level will be highly appreciated for the treatment of type 2 diabetes.

Moreover, they produce clinical effect by acting through not only SUR but also PPARγ [13–15]. It was reported that glimepiride and glibenclamide activate endogenous PPARγ in adipocytes. Tolbutamide was reported to exhibit PPARγ binding pattern [14]. So that, some sulfonylurea compounds can activate both SU and PPARγ receptors. Pharmacophore model for sulfonylurea acting drugs was designed to comprise three lipophilic centers separated by amidic and anionic linkers [16] (Fig. 1**A**).

Peroxisome proliferator-activated receptors gamma (PPARγ) is a well-characterized member of the PPAR subfamily [17]. It has a crucial role in diabetes treatment through increasing insulin sensitizing by different tissues [18]. The essential pharmacophoric features of PPARγ agonist are an acidic head, a linker attached to an aromatic scaffold (spacer group), another linker, and a hetero-aromatic lipophilic tail (Fig. 1**B**) [19]. Thiazolidinediones (TZDs) such as rosiglitazone **III**, pioglitazone **IV** are well-known PPARγ agonists (Fig. 1**B**) [20,21].

In addition some phthalimide derivatives **V** and **VI** [22] have been reported to exhibit strong and hypoglycemic effect (Fig. 1**C**). So, in this work, we report the synthesis of new phthalimide derivatives bearing

* Corresponding authors at: Pharmaceutical Chemistry Department, Faculty of Pharmacy (Boys), Al-Azhar University, Cairo 11884, Egypt.
E-mail addresses: malzahaby@yahoo.com (M.A. El-Zahabi), Ibrahimeissa@azhar.edu.eg (I.H. Eissa).

https://doi.org/10.1016/j.bioorg.2019.103115
Received 11 May 2019; Received in revised form 29 June 2019; Accepted 9 July 2019
Available online 10 July 2019

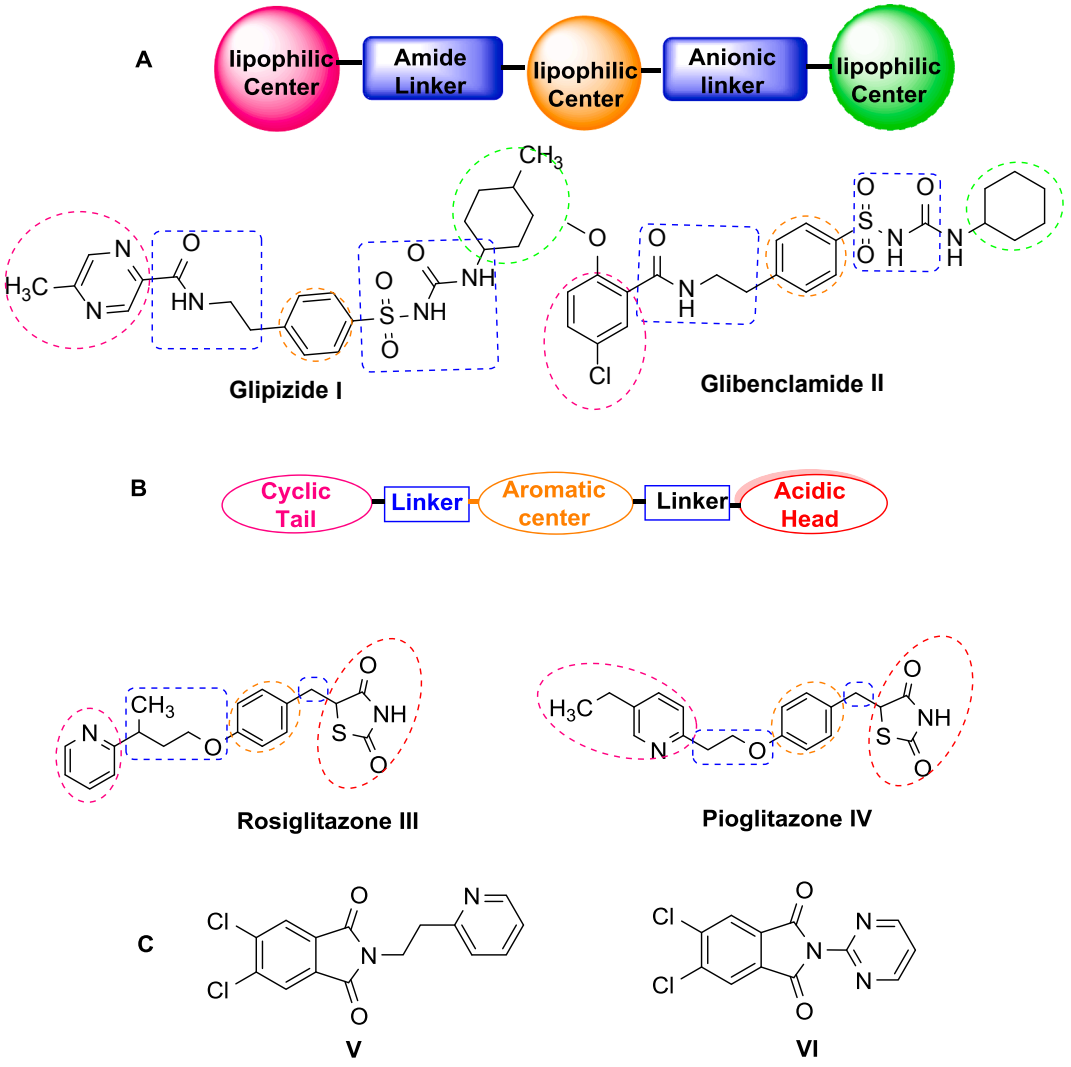

Fig. 1. (A) Pharmacophoric features of sulfonylurea agonists (B) Pharmacophoric features of PPARγ agonists (C) Reported anti-hyperglycemic phthalimides.

sulfonylurea moieties, with the aim of reaching new compounds with dual agonistic activities against PPARγ and SUR. It worth mentioning that Weber *et al* [23,24] had synthesized phthalimide derivatives bearing sulfonylurea moieties having hypoglycemic effect, but unfortunately they didn't reported the PPARγ agonistic activities of the synthesized compounds.

1.1. Rationale

As an extension for our previous works [25,26], and depending on ligand based drug design approach [27–29], we modified the well-known drug; glibenclamide to produce potent anti-hyperglycemic agents with dual agonistic activities against PPARγ and SUR. The modified compounds were designed to possess the essential pharmacophoric features of SUR and PPARγ agonists.

The acidic head required to PPARγ agonistic activity, has been replaced by sulfonylurea moiety. They form hydrogen bonds with influencing residues of the protein active site (Ser289, His323, His449 and Tyr473) [30]. Aromatic and aliphatic substitutions on sulfonylurea moiety act as a lipophilic center required to SUR agonists. Moreover, NH group of sulfamoyl moiety is acidic (pKa = 4.9–6.5) and there for completely ionized at physiological pH [31]. This ionization produces an anionic linker which contributes significantly to SUR agonistic affinity [16]. Sulfonyl (SO_2) group acts as one atom spacer between an acidic head and aromatic group. This is considered as optimal length for PPARγ agonistic activity. Para-disubstituted phenyl group acts as an aromatic scaffold (spacer group) which is required for optimal PPARγ agonism [32], in addition to its role as lipophilic center for SUR agonists. Several linkers between lipophilic tail and an aromatic scaffold (spacer group) have been synthesized to study SAR of the new compounds. Finally, phthalimide nucleus was used as lipophilic tail and lipophilic center required for PPARγ and SURs agonistic activities, respectively.

In this work, it was decided to modify its structure by such a way that the amidic function is incorporated to a bulky heterocyclic system, namely phthalimide nucleus, with the aim to explore the effects of this modification on the hypoglycemic action. One more important point deserves mentioning is substituting the free rotating amide function of glibenclamide prototypic compound with the restrictedly rotated imide nitrogen which will be a part of the phthalimide moiety. It is of interest also to try zero, one or two methylene groups as a spacer between the phenyl sulfonyl group and the phthalimide ring in order to study the effect of the different conformational orientation on the hypoglycemic activity and shed some light about the structure activity relationship of such interesting design and promising class of compounds. Moreover, a chloro group at the 3-position of the phthalimide moiety will be important by mimicking the glibenclamide and would be important to compare with the unsubstituted ring analogs. Toward that goal, it was thought worthwhile to design and synthesize three novel analogs (Targets **A**, **B** and **C**) (Fig. 2) to evaluate them as hypoglycemic agents.

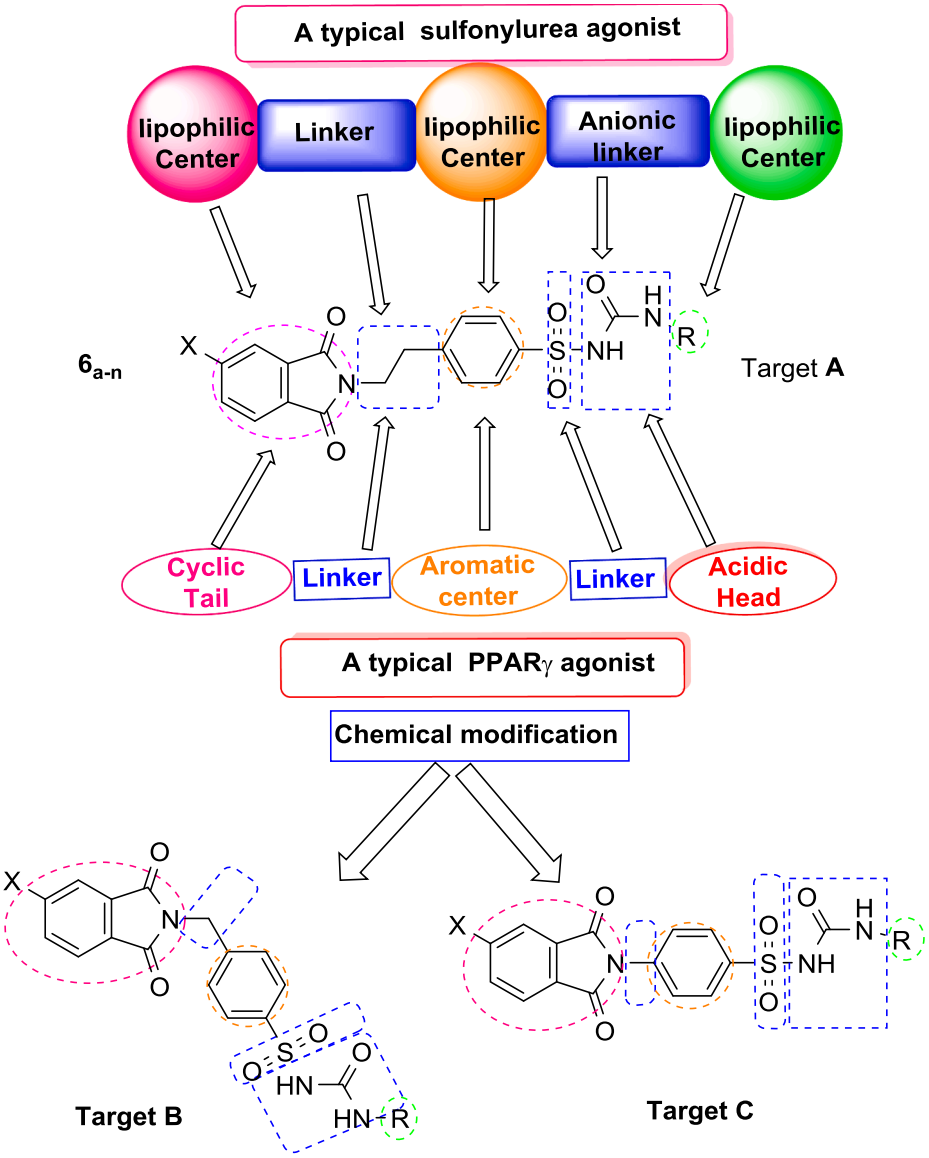

Fig. 2. The synthesized targets A, B and C with basic pharmacophoric features of SUR and PPARγ.

2. Results and discussion

2.1. Chemistry

The synthesis of the target compounds is depicted in Schemes 1–3. Two methods were adopted to synthesize the starting key compounds $\mathbf{3_{a-f}}$ [33–35]. The first one was reported by Santos *et al* [33] where, phthalic anhydride was allowed to react with benzene sulfonamide derivatives namely, 4-aminobenzenesulfonamide $\mathbf{2_a}$, 4-(amino methyl) benzene sulfonamide $\mathbf{2_b}$ and 4-(2-aminoethyl)benzene sulfonamide $\mathbf{2_c}$ in acetic acid. This method faced some problems such as long reaction time (24 h) and the low yield of the product. A modification was adopted to prepare the desired key compounds $\mathbf{3_{a-f}}$ via substituting acetic acid by DMF and Na_2CO_3 mixture, thus reduced the reaction time from 24 h to few hours and pouring the reaction mixture on acidic ice-cold water instead of evaporation under vacuum. Such modification showed better yields than the reported procedure. Anhydrous Na_2CO_3 was used in this method because 4-aminomethylbenzenesulfonamide $\mathbf{2_b}$ and 4-(2-aminoethyl) benzene sulfonamide $\mathbf{2_c}$ were available as HCl salts (Scheme 1).

Treating compound $\mathbf{3_f}$ with ethyl chloroformate in refluxing acetone in the presence of catalytic amount of anhydrous Na_2CO_3 afforded the intermediate **4** in poor yield (40%), which upon reaction with cyclohexyl amine in toluene resulted in the target product **5** in poor yield too (30%) (Scheme 2). The ^{1}H NMR spectrum of **4** showed a typical quartet-triplet pattern for the ethyl ester, the triplet signal appeared at 1.05–1.08 ppm while the quartet one was observed at 3.95–3.99 ppm. Also, this group disappeared in the ^{1}H NMR spectrum of compound **5** and the protons of cyclohexyl amine moiety appeared in the expected regions of the spectrum. Compound **5** was synthesized by another route reported through a one pot reaction. In this method, the sulfonamide $\mathbf{3_f}$ was allowed to react with Na_2CO_3 in acetone overnight then the reaction mixture was treated with cyclohexyl isocyanate to get the target compound in good yields (76%) [23,24] (Scheme 2).

Consequently, compounds $\mathbf{6_{a-n}}$ were synthesized in analogy to the one pot reaction (Scheme 3).

2.2. Biology

2.2.1. In vivo anti-hyperglycemic activity

The *in vivo* anti-hyperglycemic activity of the synthesized compounds was determined against streptozotocin-induced hyperglycemic rats using anti-hyperglycemic assay [36,37]. Glibenclamide as one of the most active anti-diabetic sulfonylurea drugs, was used as positive

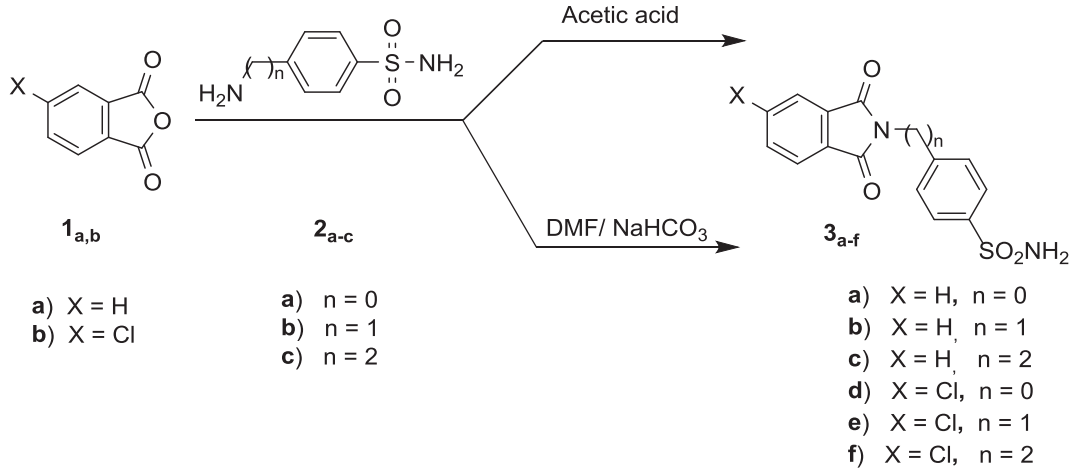

Scheme 1. Synthesis of target compounds $\mathbf{3}_{\mathbf{a\text{-}f}}$.

control. The results were reported as % reduction of blood glucose level (Table 1 & Fig. 3). Glibenclamide significantly decreased the blood glucose level by 29.3%. Compounds $\mathbf{6_c}$, $\mathbf{6_d}$, $\mathbf{6_g}$, $\mathbf{6_h}$, $\mathbf{6_j}$ and $\mathbf{6_k}$ induced significant reduction in the blood glucose levels of diabetic rats ranging from 24.43 to 21.43%. These compounds can be arranged in a descending order according to their relative potency to that of glibenclamide as follows: $\mathbf{6_k} > \mathbf{6_j} > \mathbf{6_d} > \mathbf{6_c} > \mathbf{6_g} > \mathbf{6_h}$. All the tested compounds were less potent than glibenclamide as anti-hyperglycemic agents.

2.2.2. Oral glucose Tolerance test (OGTT)

Induction of diabetes significantly increased the total AUC recording 71130 Vs 17153 mg/dL.min (+314%) of the normal control rats (Table 2). Glibenclamide induced significant reduction in the total AUC compared to the diabetic control recording 53,320 Vs 71130 mg/dL·min. The other tested compounds produced promising change the AUC. This means that these compounds have an extra pancreatic effect (PPARγ agonistic activity). They affect the glucose utilization by the muscles or the liver and may exert their effect through increasing of insulin sensitization.

2.3. Molecular modeling

Depending on availability of PPARγ crystal structures in the Protein Data Bank, receptor based drug design (docking) technique [38–42] was used to investigate the binding pattern of the synthesized compounds with the prospective target, PPARγ. On the other hand, the crystal structure of SUR is not available, so that, ligand based drug design (pharmacophore) technique [43,44] was used to predict proposed agonistic activity of the synthesized compounds against SUR.

2.3.1. Docking studies

Crystallographic structure of PPARγ was retrieved from Protein Data Bank [PDB ID- 1FM6, resolution 2.1 Å] (http://www.pdb.org), and considered as a target for docking simulations. The docking analysis was performed using MOE [45] software to evaluate the free energies and binding mode of the designed molecules against PPARγ. At first, the crystal structure of PPARγ was prepared by removing water molecules and retaining only one chain and its co-crystallized ligand, rosiglitasone. Then, the protein structure was protonated, and the hydrogen atoms were hided. Next, the energy was minimized, and the binding pocket of the protein was defined.

The 2D structures of the synthesized compounds and reference ligands (rosiglitazone and glibenclamide) were sketched using ChemBioDraw Ultra 14.0 and saved as MDL-SD format. Then, the saved file was opened using MOE and 3D structures were protonated. Next, energy minimization was applied. Before docking the synthesized compounds, validation of the docking protocol was carried out by

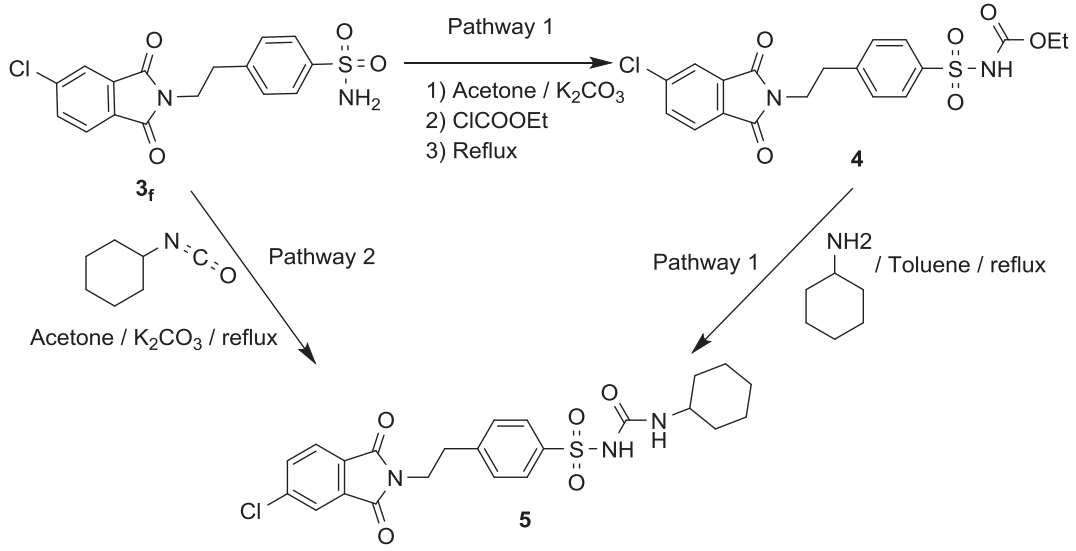

Scheme 2. Synthesis of target compound **5**.

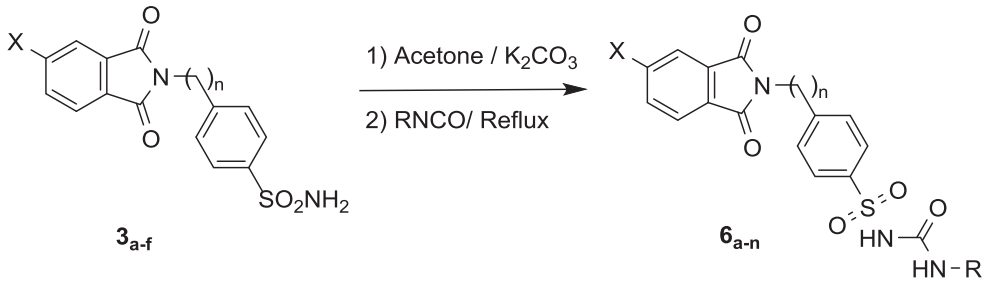

a) X = H, n = 0, R= cyclohexyl
b) X = H, n = 0, R= n-butyl
c) X = H, n = 1, R= cyclopentyl
d) X = H, n = 1, R= n-butyl
e) X = H, n = 2, R= cyclopentyl
f) X = H, n = 2, R= n-butyl
g) X = Cl, n = 0, R= cyclohexyl
h) X = Cl, n = 0, R= cyclopentyl
i) X = Cl, n = 0, R= n-butyl
j) X = Cl, n = 1, R= cyclopentyl
k) X = Cl, n = 1, R= cyclohexyl
l) X = Cl, n = 1, R= n-butyl
m) X = Cl, n = 2, R= cyclopentyl
n) X = Cl, n = 2, R= n-butyl

Scheme 3. Synthesis of target compounds $\mathbf{6_{a-n}}$.

Table 1
In vivo reduction in blood glucose levels for 7 days, in an equamolar doses (5 mg/kg) of the synthesized compounds and glibenclamide.

Rats and treatment	Blood glucose level (mg/dL)[a]		Reduction in blood glucose level (mg/dL)	Reduction in blood glucose level (%)	Relative potency to glibenclamide (RP)
	Before treatment	After treatment			
Normal Rats	116.1 ± 11.08	105.5 ± 7.91	10.6	9.20	–
Diabetic Rats	471.2 ± 53.29	450.8 ± 28.79	20.4	4.32	–
Glibenclamide	470.6 ± 22.77	332.8 ± 25.23	137.8	29.28	1
5	359.7 ± 9.10	301.2 ± 10.64	58.7	16.31	0.56
$\mathbf{6_a}$	385.6 ± 12.19	319.3 ± 15.20	66.6	17.27	0.59
$\mathbf{6_b}$	390.3 ± 10.19	338.9 ± 10.20	51.4	13.42	0.46
$\mathbf{6_c}$	447.8 ± 47.55	352.2 ± 63.03	95.6	21.43	0.73
$\mathbf{6_d}$	498.2 ± 19.84	390.6 ± 22.58	107.6	21.59	0.74
$\mathbf{6_e}$	501.4 ± 6.816	402.4 ± 20.10	99.0	19.74	0.67
$\mathbf{6_f}$	487.8 ± 30.05	447.2 ± 45.58	40.6	8.32	0.28
$\mathbf{6_g}$	263.1 ± 74.99	207.2 ± 11.65	55.9	21.24	0.73
$\mathbf{6_h}$	271.8 ± 70.27	214.1 ± 84.08	57.7	21.22	0.73
$\mathbf{6_i}$	582.4 ± 12.54	521.6 ± 18.75	60.8	10.43	0.36
$\mathbf{6_j}$	551.4 ± 6.816	422.4 ± 20.10	129.0	23.39	0.80
$\mathbf{6_k}$	525.6 ± 20.616	397.2 ± 13.52	128.4	24.43	0.83
$\mathbf{6_l}$	376.1 ± 18.71	301.3 ± 15.60	74.8	19.88	0.67
$\mathbf{6_m}$	466.75 ± 7.66	416.7 ± 10.25	50	10.71	0.37
$\mathbf{6_n}$	503.1 ± 40.80	450.8 ± 26.86	52.3	10.39	0.35

[a] All data within 10% (n = 3).

running the simulation only using the co-crystallized ligand and low RMSD between docked and crystal conformations. The molecular docking of the synthesized compounds and the co-crystallized ligand was performed using a default protocol. In each case, 10 docked structures were generated using genetic algorithm searches.

The PPARγ cavity consists of three main parts; an entrance, arm I and arm II. The arm I contains four polar residues, Tyr473, Ser289, His449 and His323, involved in hydrogen bonding. Arm II comprises Leu353, Ile 341, Ile281 and Val339 while the entrance consists of Arg288, Ser342, Leu330 and Leu333 [30] (Fig. 4).

The results of docking studies revealed that the synthesized compounds exhibited similar orientations inside the putative binding sites of PPARγ. The designed members showed good binding energies ranging from −14.00 to −26.63 kcal/mol (Table 3).

The proposed binding mode of the co-crystallized ligand, rosiglitazone, showed an affinity value of − 27.89 kcal/mol. Thiazolidinedione moiety was oriented in the polar arm I of the target receptor. Hydrogen bonding interaction with a distance of 2.51 Å was observed between the acidic hydrogen of the imide group and Ser289. The nitrogen atom of pyridine group formed one hydrogen bond with Ser342 with a distance of 2.34 Å. The pyridine moiety occupied the area of the hydrophobic pocket forming pi-cation interaction with Arg288, besides two pi-pi and pi-sigma interactions. These results were in agreement with the reported data [30] (Fig. 5).

Compound $\mathbf{6_j}$ as representative example exhibited a binding mode similar to that of rosiglitazone, with affinity value of − 26.63 kcal/mol.

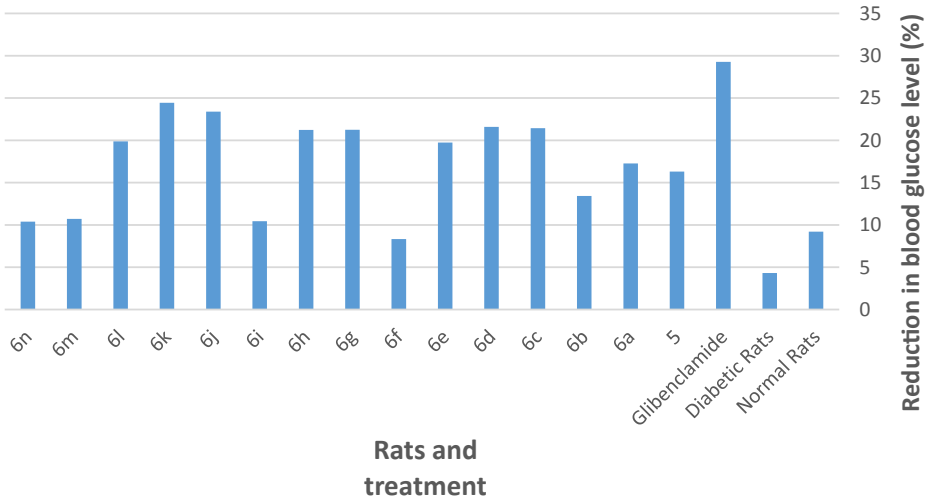

Fig. 3. Antihyperglycemic effect of the tested compounds.

Table 2
Total area under the curve (AUC) after glucose loading in normal and diabetic rats pretreated with vehicle, glibenclamide and the synthesized compounds in an equimolar dos of 5 mg/kg.

Treatment	Total AUC (mg/dl. min)	Reduction in AUC (%)
Normal rats	17153 ± 123.33	NR[a]
Diabetic Rats	71130 ± 326.24	NR[a]
Glibenclamide	53320 ± 432.23	25
6_c	57400 ± 5423.27	19
6_d	56440 ± 6534.25	20
6_g	58810 ± 2354.12	17
6_h	58610 ± 5423.17	17
6_j	55260 ± 3329.17	22
6_k	57350 ± 4012.32	19
6_l	58240 ± 4135.38	18

[a] No reduction in AUC

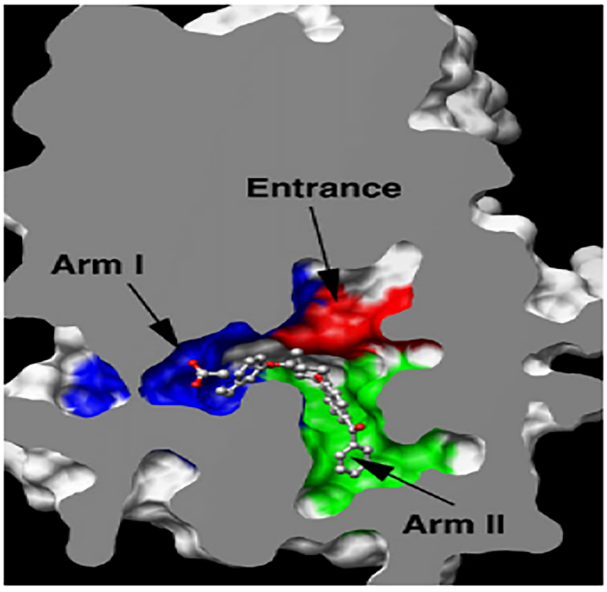

Fig. 4. PPARγ cavity composed of three main parts arm I, arm II and entrance [30].

The sulfonylurea moiety was oriented in the polar arm I of PPARγ and formed two hydrogen bonds with Ser289 (OH) and Cys285 (C═O) via C═O and NH groups of urea moiety, with distance of 2.65 and 2.58 Å, respectively. Phthalimide moiety was oriented in the hydrophobic entrance forming pi-pi and pi-cation interactions (Fig. 6). Mapping surface technique was carried out to show compound **6_j** occupying the active pocket of PPARγ (Fig. 7).

Table 3
The docking binding free energies of the synthesized compounds.

Comp. No.	Binding free energy (kcal/mol)	Comp. No	Binding free energy (kcal/mol)
5	−14.19	**6_i**	−21.75
6_a	−14.00	**6_j**	−26.63
6_b	−20.41	**6_k**	−22.64
6_c	−25.11	**6_l**	−23.76
6_d	−25.12	**6_m**	−25.61
6_e	−21.26	**6_n**	−19.84
6_f	−19.63	**Glibenclamide**	−24.11
6_g	−14.44	**Rosiglitazone**	−27.89
6_h	−19.54		

The proposed binding mode of compound **6_m** (affinity value of −25.61 kcal/mol) was virtually the same as that of rosiglitazone, where its sulfonylurea moiety directed into the polar arm I. It formed two hydrogen bonds with Tyr473 (OH) and Tyr327 (OH) via NH and C═O groups of urea moiety, with distance of 2.42 and 2.77 Å, respectively. The heterocyclic phthalimide moiety was oriented in the hydrophobic entrance forming pi-pi and pi-cation interactions with Arg288 (Fig. 8).

2.3.2. Pharmacophore studies

2.3.2.1. Generation of 3D-pharmacophore model. A 3D pharmacophore model was generated and validated using a set of thirty one compounds containing a sulfonylurea scaffold [25,26,46] (Fig. 15). The generated model was used as 3D look inquiry for determination the agonistic activities of the synthesized members against SUR.

In general, ten hypotheses were generated as shown in Table 4. Most of hypotheses involved the following features; Hydrogen bond acceptors (HBA), hydrogen bond donor (HBD), hydrophobic aliphatic (HA) and ring aromatic (RA). All of the generated hypotheses have cost differences over than 60 bits and high correlations indicating their stability. The total cost of some hypotheses is close to the fixed cost and very different to the null cost value, indicating good hypotheses.

Hypo-1 (the one with the highest correlation, the lowest RMS and the lowest total cost) was the optimal one and used for further analyses. The RMS value of 1.01, correlation coefficient of 0.89 and cost difference of 115.14 (Table 4). It consisted of four features (HBA, HBD, HA, RA). The spatial arrangement and the distances between the

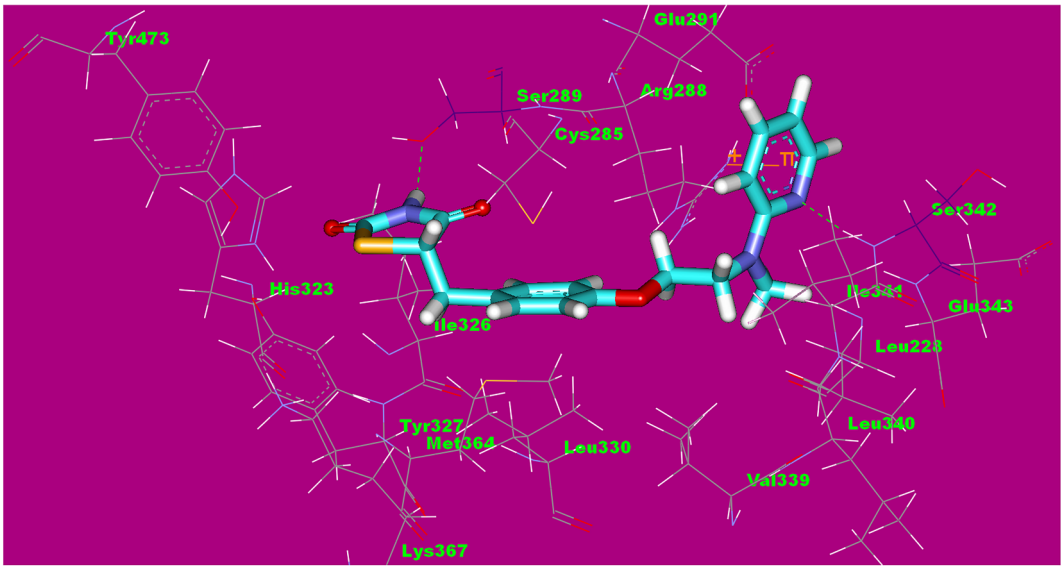

Fig. 5. Binding mode of rosiglitazone forming hydrogen bond (green dot) between its polar head and Ser289.

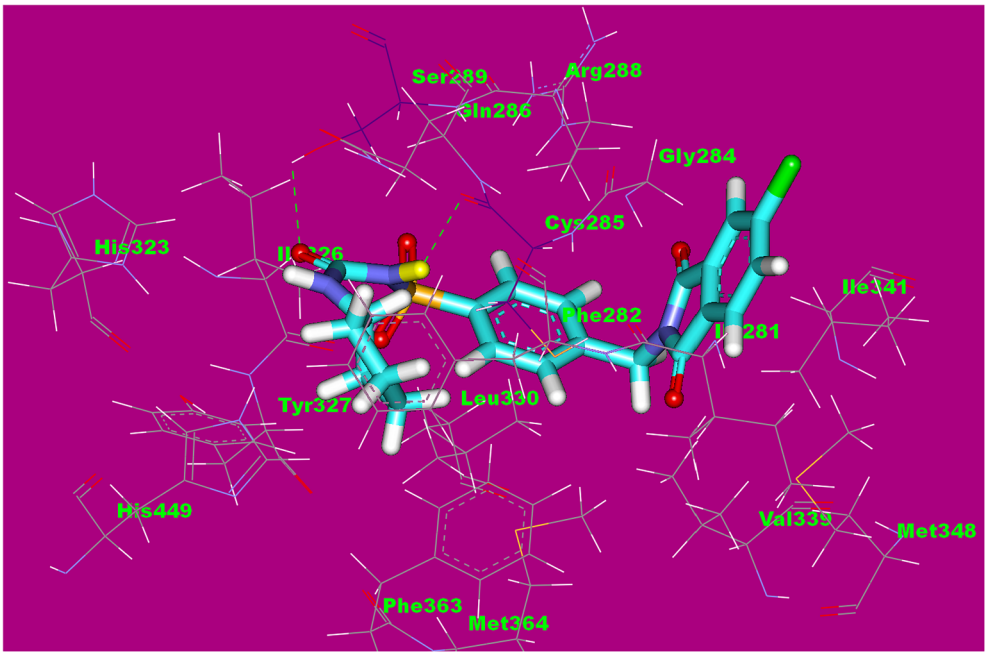

Fig. 6. Compound $\mathbf{6_j}$ docked into the active site of PPARγ. The sulfonylurea moiety formed two hydrogen bonds (green) with Ser289 and Cys285 residues.

pharmacophore features of hypo-1 are demonstrated in Fig. 9.

In order to assess the Hypo-1 predictability, experimental and estimated activities of the training set compounds were compared. The results indicated that there is marked consistency between experimental and predicted activity values for all test compounds. This indicates that the pharmacophore Hypo-1 classifies the training set compounds correctly (Table 5).

2.3.2.2. Validation of Hypo-1 pharmacophore model. Validation processes were carried out to test the ability of the built model to distinguish active structures and anticipate their activities precisely. Two methods were done to validate the hypo-1; test set activity prediction and mapping of glibenclamide as an external reference of the generated pharmacophore.

2.3.2.2.1. Test set activity prediction. Test set of ten compounds was subjected to the same protocol of training set to verify the ability of the generated pharmacophore model (hypo-1) to predict the activities of the new synthesized compounds. The obtained results showed that hypo-1 can classify the active and inactive compounds correctly. Experimental and estimated activities and fit values of the test set were listed in Table 6.

2.3.2.2.2. Mapping of glibenclamide. Glibenclamide was mapped with the generated pharmacophore (hypo-1) and demonstrated a high fit value of 7.98. The chloro phenyl moiety completely fitted with RA, the sulfonyl group fitted with HBA, the central phenyl ring fitted with RA and the NH of amide linker fitted with HBD (Fig. 10).

2.3.2.3. Estimation of designed molecules. The validated pharmacophore model (Hypo-1) was used to estimate the activities of the synthesized members according to the degree of fitting with Hypo-1. The estimated activities and fit values of the synthesized compounds were listed in Table 7. It was observed that most of the synthesized compounds have

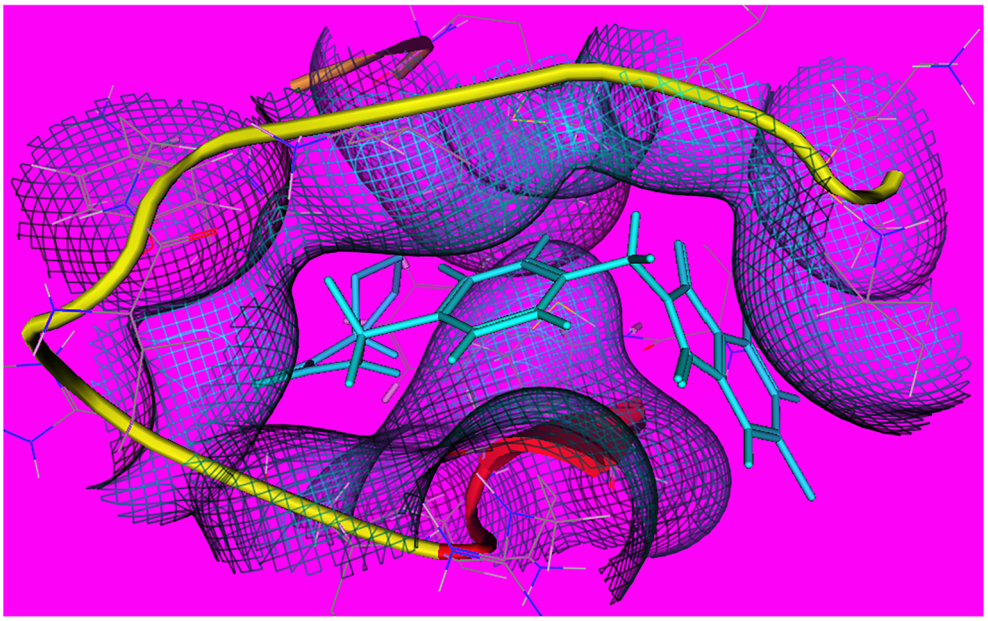

Fig. 7. Mapping surface showing compound 6j occupying the active pocket of PPARγ.

high fit values toward Hypo1, indicating promising SUR agonistic activities. Compounds **6c**, **6j**, **6k**, **6l**, and **6n** showed the highest fit values against the generated pharmacophore model Mapping of three designed compounds (**6j**, **6k** and **6l**) on the generated pharmacophore (Hypo1) was demonstrated in Figs. 11–13, respectively. It was noted that the mapping pattern of these compounds is as the same as that of glibenclamide.

In order to probe the similarity between the 3D structures of one of the synthesized compounds **6e** and glibenclamide; flexible alignment was carried out via molecular overlay protocol using discovery studio 2.5 software [44]. Compound **6e** showed a distinct similar pattern with significant fairly alignment with glibenclamide (Fig. 14).

2.3.3. QSAR studies

In our previous work [26], two QSAR models were generated and validated to identify the substituents effect on the PPARγ binding affinity and insulin-secreting ability. The generated QSAR models were summarized in Eqs. (1) and (2) which describe PPARγ binding affinity and insulin-secreting ability, respectively.

$$pIC_{50} = -9.489 + 8.748ALogP - 1.691MR + 2.033MPSA + 2.267PPSA1 - 2.264WPSA1 \quad (1)$$

$$pEC_{50} = 1.821 - 5.579MR - 0.256HBA - 0.734CHI - 1 - 5.115PPSA - 1 + 3.584WPSA - 2 + 0.487Shad - Y \quad (2)$$

where, ALogP: partition coefficient, MR: molar refractivity, MPSA: molecular polar surface area, PPSA1: partial positive surface area, WPSA1: surface-weighted charged partial surface areas, HBA: hydrogen bond acceptors, CHI-1: Kier's molecular connectivity, Shad-Y: shadow_Y length.

In this work, we calculated predicted pIC_{50} ($-\log IC_{50}$) and pEC_{50} ($-\log EC_{50}$) depending on the generated QSAR models. Then, the predicted PPARγ binding affinity (IC_{50}) and insulin-secreting ability (EC_{50}) were calculated from Eqs. (3) and (4), respectively (Table 8).

$$IC_{50} = 10^{-pIC50} \quad (3)$$

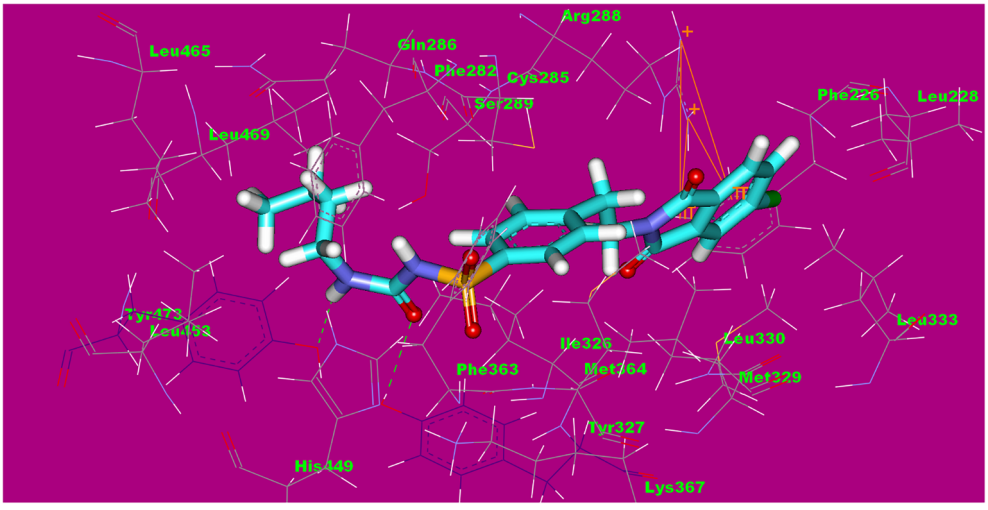

Fig. 8. Compound **6m** docked into the active site of PPARγ. The sulfonylurea moiety formed two hydrogen bonds (green) with Tyr473 and Tyr327residues.

Table 4
Statistical significance, predictive power and features of the top-10 pharmacophore hypotheses derived from the training set of molecule.

Hypo.	Total cost	Cost difference[a]	RMS[b]	Correlation	Features[c]	Max. fit
Hypo 1	115.14	96.70	1.01	0.89	HBA, HBD, HA, RA	9.35
Hypo 2	117.77	94.07	1.02	0.78	HBA, HBD, HA, RA	8.22
Hypo 3	119.14	92.70	1.27	0.62	HBA, HBD, RA	6.53
Hypo 4	122.37	89.47	1.63	0.61	HBA, HBA, HBA, HAr, RA	5.01
Hypo 5	124.69	87.15	1.10	0.59	HBD, HBD, HBD, HA	6.20
Hypo 6	121.73	90.11	1.14	0.72	HBA, HBA, HA, RA	8.19
Hypo 7	122.61	89.23	1.21	0.67	HBA, HBA, HBD, HA	6.76
Hypo 8	123.38	88.46	1.28	0.62	HBA, HBA, HBD, HA	7.52
Hypo 9	123.42	88.42	1.17	0.70	HBA, HBA, HA, RA	8.04
Hypo 10	123.51	96.70	1.21	0.67	HBA, HBA, HBD, HA	7.52

[a] Cost difference is the difference between null cost and total cost. Null cost = 214.84 bit.
[b] RMS, root mean square deviation, the deviation of log estimated activities from log experimental activities normalized by log uncertainty.
[c] Abbreviation used for features; HBA: hydrogen bond acceptor, HBD: hydrogen bond donor, HA: hydrophobic aliphatic, HAr: hydrophobic aromatic, RA: ring aromatic.

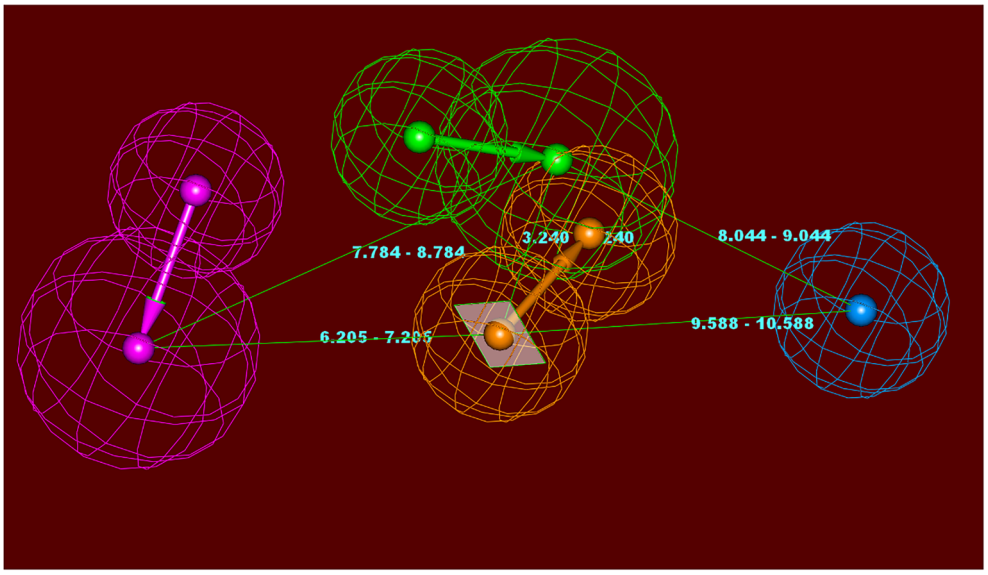

Fig. 9. Hypo 1 with four features; green (HBA), blue (HA), purple (HBD) and brown (RA). The distance constraint between pharmacophore features is reported in angstroms.

$$EC_{50} = 10^{-pEC50} \quad (4)$$

2.3.4. *In silico ADMET analysis*

Prediction of ADMET (absorption, distribution, metabolism, excretion and toxicity) for the synthesized compounds and reference drugs (pioglitazone and glibenclamide) was carried out using Discovery studio 2.5. Predicted ADMET for all the tested molecules are listed in Table 9.

From the data, it was found that the synthesized compounds showed low BBB penetration. Consequently, these compounds were expected to be safe to central nervous system. Moreover, many of the synthesized compounds were expected to have considerable human intestinal absorption. Additionally, the inhibitory and non-inhibitory behaviors of the synthesized compounds on Cytochrome P450 2D6 enzyme were also detected via the CYP2D6 score prediction. It was predicted that most of the synthesized compounds are non-inhibitors of CYP2D6. Hence, these compounds may not have hepatic adverse effects. Additionally, the closer the hepatotoxicity scores to one, the more probability to be toxic, while the closer the hepatotoxicity scores to zero, the more probability to be nontoxic [47,48]. About one half of the synthesized compounds were found to have hepatotoxicity probability values below 0.5. Hence these derivatives are likely to be non-hepatotoxic. While the other compounds were found to have hepatotoxicity probability values ranging above 0.5. This indicates that these derivatives are likely to possess hepatotoxicity. The model of plasma protein binding (PPB) predicts the binding ability of a compound to plasma proteins. The majority of the synthesized members have PPB level equal to one. So, there is a good chance for these compounds to reach the desired targets easily. It is well known that a lot of drug candidates under clinical tests have failed due to their absorption properties problems [49]. Computational examination of the synthesized compound showed that their ADMET aqueous solubility logarithmic levels are as like as that of the reference drugs.

2.4. *Structure-activity relationship (SAR)*

The % reduction in blood glucose levels of compounds **5**, $\mathbf{6_g}$ and $\mathbf{6_k}$ incorporating cyclohexyl moiety were found to be higher than that of corresponding members $\mathbf{6_m}$, $\mathbf{6_h}$ and $\mathbf{6_j}$ incorporating cyclopentyl group, and the latter were found to be more active than that with *n*-butyl substitution as compounds $\mathbf{6_n}$, $\mathbf{6_i}$ and $\mathbf{6_n}$, indicating that cyclohexyl derivatives are more advantageous than cyclopentyl ones which are more active than *n*-butyl ones. Cyclic structure of cyclohexyl and cyclopentyl may produce ideal fitting with the hydrophobic pocket of PPARγ.

The increased % reduction in blood glucose levels of compounds $\mathbf{6_{j-l}}$ than those of their corresponding members **5**, $\mathbf{6_{m,n}}$, and $\mathbf{6_{g-i}}$, indicated

Table 5
Experimental and estimated activities of the training set compounds based on pharmacophore model hypo 1.

Comp.	Exp.[a] (μM)	Est[b] (μM)	Fit value[c]	Error[d]
$\mathbf{7_a}$	0.01	0.01	8.81	−1.06
$\mathbf{7_b}$	0.01	0.02	6.57	1.48
$\mathbf{7_c}$	0.02	0.02	8.47	−1.18
$\mathbf{7_d}$	0.03	0.03	8.34	−1.02
$\mathbf{7_e}$	0.01	0.03	6.27	2.51
$\mathbf{8_a}$	0.08	0.03	5.27	−2.30
$\mathbf{8_b}$	0.03	0.04	6.22	1.10
$\mathbf{9_a}$	0.03	0.04	7.22	1.26
$\mathbf{9_b}$	0.03	0.04	7.20	1.33
$\mathbf{10_a}$	0.04	0.04	9.16	−1.02
$\mathbf{10_b}$	0.02	0.04	6.14	2.00
$\mathbf{11_a}$	0.03	0.04	7.14	1.34
$\mathbf{11_b}$	0.04	0.05	7.12	1.05
$\mathbf{11_c}$	0.03	0.05	6.10	1.45
$\mathbf{11_d}$	0.03	0.05	6.10	1.92
$\mathbf{12_a}$	0.10	0.05	6.10	−1.95
$\mathbf{12_b}$	0.09	0.05	6.07	−1.69
$\mathbf{12_c}$	0.09	0.05	6.06	−1.77
$\mathbf{12_d}$	0.10	0.06	6.03	−1.73
$\mathbf{12_e}$	0.04	0.06	7.01	1.36

[a] Experimental activity value.
[b] Estimated activity value.
[c] Fit value calculated by geometry fitting between the hypothesis and the compound; the higher value, the better fit.
[d] Error factor calculated as the ratio of the measured activity to the estimated activity or the inverse if the estimated activity is greater than the measured activity. If measured activity is greater than the estimated activity, the error factor is negative and vice versa.

Table 6
Experimental and estimated activities and fit values of the test set based on pharmacophore model hypo-1.

Comp.	Exp.[a] (μM)	Est[b] (μM)	Fit value[c]
$\mathbf{7_f}$	NA[d]	2.56	7.99
$\mathbf{7_g}$	0.09	0.06	7.98
$\mathbf{8_c}$	0.09	0.07	7.97
$\mathbf{9_c}$	NA[d]	3.17	6.97
$\mathbf{10_c}$	NA[d]	2.22	7.97
$\mathbf{11_e}$	NA[d]	1.97	6.96
$\mathbf{11_f}$	0.03	0.07	7.95
$\mathbf{12_f}$	0.04	0.07	7.93
$\mathbf{12_g}$	NA[d]	1.08	8.87
$\mathbf{12_h}$	0.09	0.09	7.82
$\mathbf{12_i}$	0.10	0.10	7.76

[a] Experimental activity values.
[b] Estimated activity values.
[c] Fit value indicates how well the features in the pharmacophore overlap the chemical features in the molecule.
[d] NA: not active

that one carbon spacer between phthalimide and benzensulfonamide moieties is better than that with two carbon spacer which is more active than zero carbon spacer. Flexible alignment of compound $\mathbf{6_e}$ and glibenclamide showed high structural similarity between compounds with two carbon spacer and glibenclamide. These findings may explain the high activity of compound with one and two carbon spacers than that with zero carbon spacer.

We then examined the effect of the chloro substitution at 5-position of phthalimide moiety. The activities of compounds with chloro substitution ($\mathbf{6_{g\text{-}n}}$) were better than that unsubstituted analogs (**5** and $\mathbf{6_{a\text{-}f}}$), indicating that grafting a chloro group at the 5-position is beneficial for the activity. These results were confirmed by docking scores, where most of compounds with chloro substitution showed higher binding free energies than the un-substituted ones.

3. Conclusion

In this work, we synthesized a novel series of phthalimide-sulfonylurea derivatives as modified structures of glibenclamide. The synthesized compounds were subjected to two biological tests: i) *In vivo* anti-hyperglycemic activity against STZ-induced hyperglycemic rats using glibenclamide as a reference drug, ii) Oral Glucose Tolerance Test. Compounds $\mathbf{6_c}$, $\mathbf{6_d}$, $\mathbf{6_g}$, $\mathbf{6_h}$, $\mathbf{6_j}$ and $\mathbf{6_k}$ induced significant reduction in the blood glucose levels of diabetic rats ranging from 24.43 to 21.43%. Four molecular modeling techniques (docking and pharmacophore, QSAR and ADMET) were carried out. Compounds $\mathbf{6_c}$, $\mathbf{6_d}$, $\mathbf{6_j}$ and $\mathbf{6_m}$ exhibited the highest binding free energies against PPARγ. Compounds $\mathbf{6_c}$, $\mathbf{6_j}$, $\mathbf{6_k}$, $\mathbf{6_l}$, and $\mathbf{6_n}$ showed the highest fit values against the generated pharmacophore model. The synthesized compounds showed promising estimated PPARγ binding affinities and insulin-secreting abilities toward the generated QSAR model. *In-silico* studies revealed that the synthesized compounds have considerable human intestinal absorption with low BBB penetration.

4. Experimental

4.1. Chemistry

Melting points were determined with Barnested electro-thermal melting point apparatus and were uncorrected. The IR spectra were detected using a Pye-Unicam SP-3-300 infrared spectrophotometer using potassium bromide dicks and expressed in wave number (cm^{-1}). Nuclear magnetic resonance (^{1}H NMR) spectra were done on 600 MHz Bruker Advance DPX600 spectrometer using the Me_4Si as internal reference and DMSO-d_6 or $CDCl_3$ were used as solvents. Chemical shifts (δ) are quoted in ppm. The abbreviations used are as follows: s, singlet; d, doublet; m, multiplet. All coupling constant (J) values are given in hertz. The mass spectra were carried out on Shimadzu GCMS-QP-1000EX mass spectrometer at70 eV. Elemental analyses were done on CHN analyzer and all compounds were within ± 0.5 of the theoretical values. Thin-layer chromatography (TLC) was used to monitor the reactions using TLC sheets coated with UV fluorescent silica gel Merck 60 F254 plates and were visualized using UV lamp and different solvents as mobile phases. Chemicals are Aldrich and Fluka products and are used without further purification. Compounds $\mathbf{2_a}$, $\mathbf{2_b}$ and $\mathbf{2_c}$ were prepared according to reported methods [33–35].

4.1.1. General procedure for synthesis of compounds $3_{a\text{-}f}$

Method A: A mixture of anhydrides $\mathbf{1_{a,b}}$ (1 mmol) and the appropriate benzensulfonamides (1 mmol) namely, 4-aminobenzenesulfonamide $\mathbf{2_a}$, 4-(aminomethyl)benzenesulfonamide $\mathbf{2_b}$ and 4-(2-aminoethyl) benzenesulfonamide $\mathbf{2_c}$ in acetic acid (10 ml) was heated under reflux for 24 h. The reaction mixture was cooled and the solvent was removed under vacuum. The obtained residue was filtered, dried and crystallized from ethanol to give the title compounds $\mathbf{3_{a\text{-}f}}$, respectively.

Method B: A mixture of anhydrides $\mathbf{1_{a,b}}$ (1 mmol) and the appropriate benzensulfonamides (1 mmol) namely, 4-aminobenzenesulfonamide $\mathbf{2_a}$, 4-(aminomethyl)benzenesulfonamide $\mathbf{2_b}$ and 4-(2-aminoethyl) benzenesulfonamide $\mathbf{2_c}$ in DMF (10 ml) was heated under reflux for 3–5 h. Then, the reaction mixture was poured on ice cold water. The separated solid was collected by filtration, dried and crystallized from ethanol to afford the target compounds $\mathbf{3_{a\text{-}f}}$, respectively.

4.1.1.1. 4-(5-Chlorophthalimido)benzenesulfonamide 3_d. White powder (yield 63%); m.p. 176–178 °C; IR (KBr, υ cm^{-1}): 3347, 3253 (NH_2), 3114 (C—H aromatic), 2945 (C—H aliphatic), 1709 (C=O), 1329, 1151 (SO_2);^{1}H NMR (DMSO-d_6, 600 MHz) δ (ppm): 7.54 (s, 2H, NH_2, D_2O exchangeable), 7.63–7.65 (d, 2H, Ar-H), 7.90–7.92 (d, 2H, Ar-H), 7.94–7.97 (m, 3H, Ar-H).; Anal. Calcd. for $C_{14}H_9ClN_2O_4S$ (336.00): C, 49.93; H, 2.69; N, 8.32; Found: C, 49.55; H, 2.27; N, 8.02.

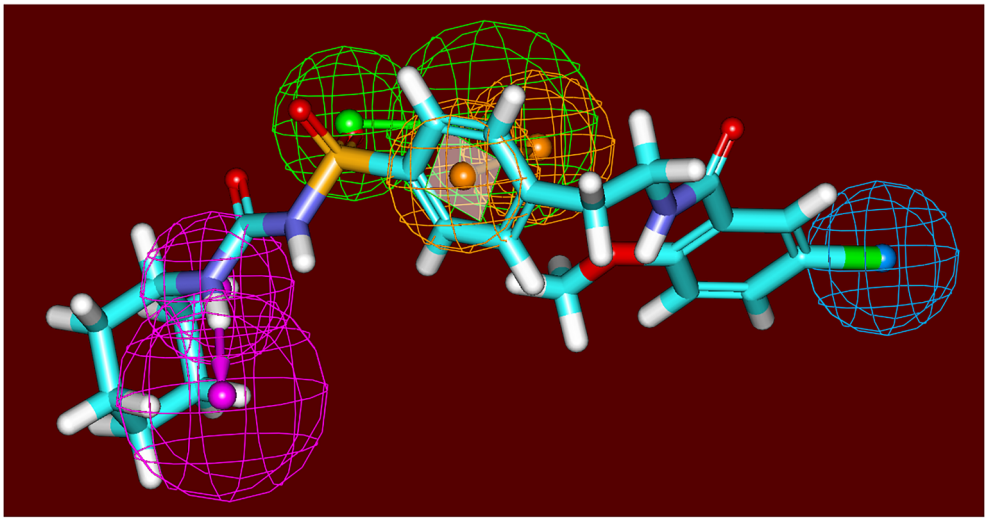

Fig. 10. Mapping of glibenclamide on the generated high ranked pharmacophore (Hypo1); green (HBA), blue (HA), purple (HBD) and brown (RA).

Table 7
Expected activities and fit values of designed compounds based on the Hypo 1 pharmacophore model.

Comp.	Est.[a] (μM)	Fit value[b]	Comp.	Est.[a] (μM)	Fit value[b]
5	0.06	7.19	$\mathbf{6_h}$	0.03	7.60
$\mathbf{6_a}$	0.10	5.80	$\mathbf{6_i}$	0.08	7.32
$\mathbf{6_b}$	0.08	7.43	$\mathbf{6_j}$	0.03	8.79
$\mathbf{6_c}$	0.07	7.66	$\mathbf{6_k}$	0.03	7.79
$\mathbf{6_d}$	0.08	6.52	$\mathbf{6_l}$	0.03	7.75
$\mathbf{6_e}$	0.06	7.64	$\mathbf{6_m}$	0.06	6.83
$\mathbf{6_f}$	0.12	7.52	$\mathbf{6_n}$	0.04	8.14
$\mathbf{6_g}$	0.10	6.62	**Glibenclamide**	0.02	8.94

[a] Estimated activity value.
[b] Fit value indicates how well the features in the pharmacophore overlap the chemical features in the molecule.

4.1.1.2. 4-(5-Chlorophthalimidomethyl)phenylsulfonamide 3e. White crystals (yield 60%); m.p. 250–252 °C; IR (KBr, υ cm^{-1}): 3356, 3257 (NH_2), 3073 (C—H aromatic), 2935 (C—H aliphatic), 1705 (C═O), 1313, 1158 (SO_2); ^{1}H NMR (DMSO-d_6, 600 MHz) δ (ppm): 4.83 (s, 2H, CH_2), 7.38 (s, 2H, NH_2, D_2O exchangeable), 7.45–7.46 (d, 2H, Ar-H), 7.75–7.76 (d, 2H, Ar-H), 7.84–7.89 (m, 3H, Ar-H); Anal. Calcd. for $C_{15}H_{11}ClN_2O_4S$ (350.01): C, 51.36; H, 3.16; N, 7.99; Found: C, 51.65; H, 3.45; N, 7.59.

4.1.1.3. 4-(2-(5-Chloro-1,3-dioxoisoindolin-2-yl)ethyl) benzenesulfonamide 3f. White crystals (yield 68%); m.p. 251–253 °C; IR (KBr, υ cm^{-1}): 3361, 3271 (NH_2), 3075 (C—H aromatic), 2930 (C—H aliphatic), 1710 (C═O), 1334, 1161 (SO_2);^{1}H NMR (DMSO-d_6, 600 MHz) δ (ppm): 2.99–3.02 (t, 2H, CH_2), 3.84–3.86 (t, 2H, CH_2), 7.33 (s, 2H, NH_2, D_2O exchangeable), 7.40–7.41 (d, 2H, Ar-H), 7.70–7.72 (d, 2H, Ar-H), 7.82–7.86 (m, 3H, Ar-H); Anal. Calcd. for $C_{16}H_{13}ClN_2O_4S$ (364.03): C, 52.68; H, 3.59; N, 7.68; Found: C, 52.25; H, 3.24; N, 7.37.

4.1.1.4. Ethyl N-[4-(5-Chlorophthalimdoethyl)phenylsulfonyl]-N'-formate 4. A mixture of 4-(5-chlorophthalimidoethyl)phenylsulfonamide $\mathbf{3_f}$ (3.64 g, 0.01 mol) and anhydrous K_2CO_3 (0.02 mol. 2.76 g) in dry acetone (100 ml) was stirred and refluxed for 8 h. At this temperature, a solution of ethyl chloroformate (1.08 g, 0.01 mol.) in dry acetone (20 ml) was added in a drop wise manner. The reaction mixture was further refluxed overnight. The solvent was then removed under vacuum and the solid residue was dissolved in water, filtered and then acidified with sufficient amount of 2 N HCl. The separated product

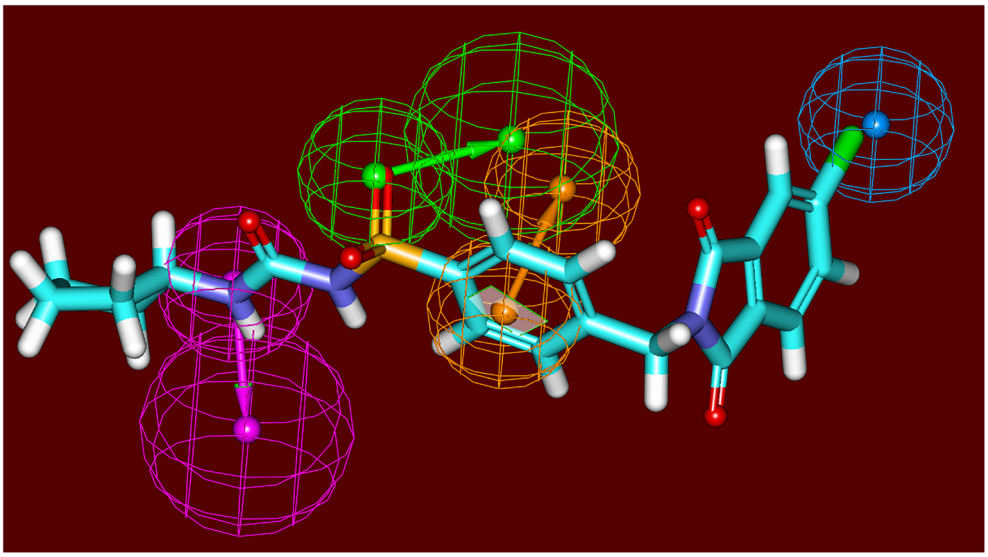

Fig. 11. Mapping of compound 6j (fit value = 8.79) on the generated high ranked pharmacophore (Hypo1); green (HBA), blue (HA), purple (HBD) and brown (RA).

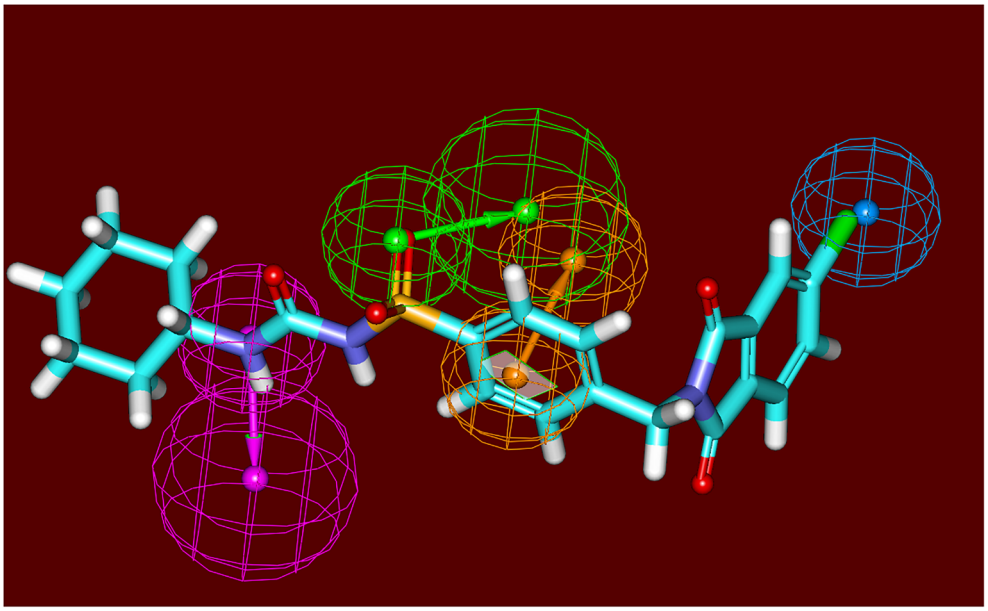

Fig. 12. Mapping of compound 6k (fit value = 7.79) on the generated high ranked pharmacophore (Hypo1); green (HBA), blue (HA), purple (HBD) and brown (RA).

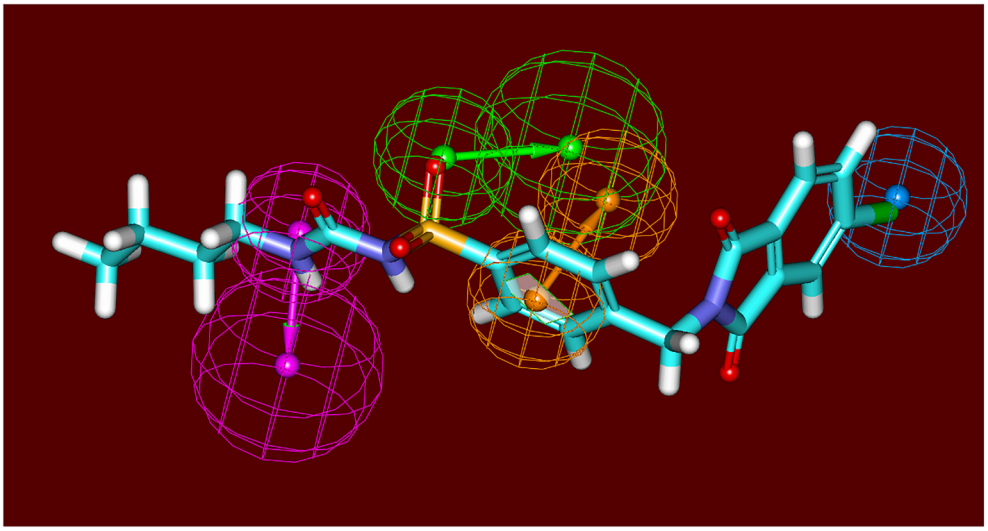

Fig. 13. Mapping of compound 6l (fit value = 7.75) on the generated high ranked pharmacophore (Hypo1); green (HBA), blue (HA), purple (HBD) and brown (RA).

was recrystallized from ethanol to get compound **4**.

White powder (yield 40%); m.p. 320–322 °C;^{1}H NMR (DMSO-d_6, 600 MHz) δ (ppm): 1.05–1.08 (t, 3H, CH_3), 3.02–3.04 (t, 2H, CH_2), 3.84–3.87 (t, 2H, CH_2), 3.95–3.99 (t, 2H, CH_2), 7.46–7.47 (d, 2H, Ar-H), 7.76–7.70 (d, 2H, Ar-H), 7.81–7.85 (m, 3H, Ar-H), 11.81 (s, 1H, NH, D_2O exchangeable); Anal. Calcd. for $C_{19}H_{17}ClN_2O_6S$ (436.05): C, 52.24; H, 3.92; N, 6.41; Found: C, 52.63; H, 3.63; N, 6.09.

4.1.1.5. General procedure for synthesis of compounds 5 and 6_{a-n}. **Method A:** To a solution of compound **4** (4.36 g, 0.01 mol) in hot toluene, cyclohexyl amine (0.93 g, 0.01 mol) was added. The solution was refluxed for 8 h at reflux temperature, then evaporated under vacuum. The solid so obtained was crystallized from ethanol to give compound **5**.

Method B: A mixture of compound $\mathbf{3_{a-f}}$ (0.05 mol) and anhydrous K_2CO_3 (0.1 mol, 13.8 g) in dry acetone (100 ml) was stirred and refluxed for 8 h. At this temperature, a solution of alkyl isocyanate in (0.075 mol) in dry acetone (20 ml) was added in a drop wise manner. The reaction mixture was further refluxed overnight. The solvent was then removed under vacuum and the solid residue was dissolved in water, filtered and then acidified with sufficient amount of 2 N HCl. The separated product was crystallized from ethanol to afford target compounds **5** and $\mathbf{6_{a-n}}$.

4.1.1.6. N-[4-(5-Chlorophthalimdoethyl)phenylsulfonyl]-N'-cylcohexylurea 5. White crystals (yield 76%); m.p. 191–192 °C; IR (KBr, υ cm^{-1}): 3328 (2NH, overlapped), 3039 (C—H aromatic), 2929, 2854 (C—H aliphatic), 1626 (C=O); ^{1}H NMR (DMSO-d_6, 600 MHz) δ (ppm): 1.05–1.13 (m, 3H, CH & CH_2), 1.15–1.23 (m, 2H, CH_2), 1.46–1.49 (d, 1H, CH), 1.56–1.58 (br,1H, CH_2), 1.61–1.63 (d, 2H, CH_2), 3.00–3.03 (t, 2H, CH_2), 3.25–3.26 (m, 1H, *N*-CH), 3.83–3.86 (t, 2H, CH_2), 6.33 (s, 1H, N**H**-CH_2, D_2O exchangeable), 7.44–7.46 (d, 2H, J = 8.4 Hz, Ar-H), 7.77–7.78 (m, 2H, J = 8.4 Hz, Ar-H), 7.82–7.93 (m, 3H, Ar-H), 10.35 (s, 1H, NH); Anal. Calcd. for $C_{23}H_{24}ClN_3O_5S$ (489.97): C, 56.38; H, 4.94; N, 8.58; Found: C, 56.77; H, 4.68; N, 8.29.

4.1.1.7. N-[4-(phthalimdo)phenylsulfonamide]-N'-cylcohexylurea 6_a. White crystals (yield 73%); m.p. 233–235 °C; IR (KBr, υ cm^{-1}):

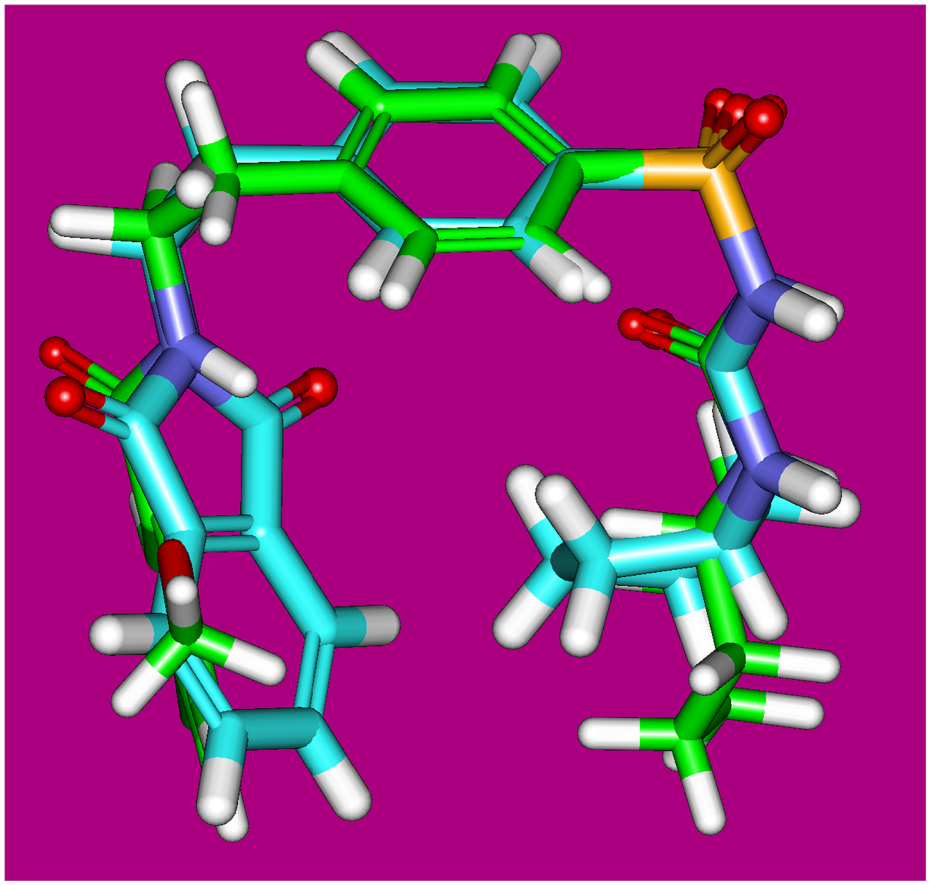

Fig. 14. Flexible alignment of compound **6_e** (faint blue) and glibenclamide (green).

Table 8
Predicted PPARγ binding affinity and insulin-secreting ability of the synthesized compounds obtained by QSAR models.

Comp.	PPARγ binding affinity		Insulin-secreting ability	
	Predicted pIC_{50} [a]	Predicted IC_{50} [b]	Predicted pEC_{50} [c]	Predicted EC_{50} [d]
5	0.69	4.87	0.65	4.48
6_a	0.62	4.13	0.30	1.99
6_b	0.47	2.98	0.13	1.34
6_c	0.51	3.21	0.30	2.00
6_d	0.49	3.10	0.95	8.97
6_e	0.52	3.28	1.07	11.69
6_f	0.61	4.05	0.20	1.57
6_g	0.59	3.91	0.90	7.99
6_h	0.44	2.73	0.04	1.11
6_i	0.46	2.91	0.39	2.46
6_j	0.41	2.58	0.15	1.40
6_k	0.59	3.89	0.19	1.56
6_l	0.46	2.89	0.42	2.64
6_m	0.47	2.95	0.49	3.12
6_n	0.59	3.87	0.48	3.02

[a] Calculated from Eq. (1).
[b] Calculated from Eq. (3) ($IC_{50} = 10^{-pIC50}$).
[c] Calculated from Eq. (2).
[d] Calculated from Eq. (4) ($EC_{50} = 10^{-pEC50}$).

3330 (2NH, overlapped), 3041 (C—H aromatic), 2929, 2854 (C—H aliphatic), 1625 (C═O); ^{1}H NMR (DMSO-d_6, 600 MHz) δ (ppm): 1.11–1.16 (m, 3H, CH + CH_2), 1.20–1.26 (m, 2H, CH_2), 1.49–1.51 (m, 2H, CH_2), 1.60–1.62 (m,1H, CH), 1.67–1.69 (m, 2H, CH_2), 1.66–1.68 (m, 2H, CH_2), 3.29–3.32 (m, 1H, *N*-CH), 6.46 (s, 1H, N**H**-cyclohexyl), 7.72–7.74 (dd, 2H, J = 8.4 Hz, Ar-H), 7.93–7.96 (m, 2H, Ar-H), 8.01–8.03 (m, 2H, Ar-H), 8.04–8.05 (d, 2H, J = 8.4 Hz, Ar-H), 10.50 (s, 1H, NH, D_2O exchangeable); Anal. Calcd. for $C_{21}H_{21}N_3O_5S$ (427.47): C, 59.00; H, 4.95; N, 9.83; Found: C, 59.44; H, 4.61; N, 9.52.

4.1.1.8. N-(4-phthalimdophenylsulfonamide)-N'-butylurea **6_b**. White powder (yield 71%); m.p. 220–222 °C; IR (KBr, υ cm^{-1}): 3254 (2NH, overlapped), 2932 (C—H aliphatic), 1693 (C═O); ^{1}H NMR (DMSO-d_6, 600 MHz) δ (ppm): 0.81–0.84 (t, 3H, CH_3), 1.16–1.22 (septet, 2H, CH_2), 1.29–1.34 (pentet, 2H, CH_2), 2.94–2.97 (q, 2H, CH_2), 6.54 (s, 1H, N**H**-CH_2, D_2O exchangeable), 7.71–7.72 (dd, 2H, Ar-H, J = 8.4 Hz), 7.93–7.95 (m, 2H, Ar-H), 8.00–8.03 (m, 2H, Ar-H), 8.04–8.05 (dd, 2H, Ar-H, J = 8.4 Hz), 10.65 (s, 1H, NH, D_2O exchangeable); MS (*m/z*): 401 (90%, M^+), 76(100%). Anal. Calcd. for $C_{19}H_{19}N_3O_5S$ (401.44): C, 56.85; H, 4.77; N, 10.47; Found: C, 56.43; H, 4.32;; N, 10.04.

4.1.1.9. N-[4-(phthalimdomethyl)phenylsulfonamide]-N'-cylcopentylurea **6_c**. White crystals (yield 68%); m.p. 145–146 °C; IR (KBr, υ cm^{-1}): 3340, 3254 (2NH), 2930 (C—H aliphatic), 1720 (C═O); ^{1}H NMR (DMSO-d_6, 600 MHz) δ (ppm): 1.26–1.29 (m, 2H, CH_2), 1.45–1.48 (m, 2H, CH_2), 1.54–1.57 (m, 2H, CH_2), 1.70–1.75 (m, 2H, CH_2), 3.72–3.74 (p, 1H, *N*-CH), 4.89 (s, 2H, CH_2), 6.46 (br s, 1H, N**H**-CH_2, D_2O exchangeable), 7.56–7.57 (d, 2H, Ar-H, J = 8.4 Hz), 7.78–8.00 (m, 2H, Ar-H, J = 8.4 Hz,), 7.85–7.89 (m, 2H, Ar-H), 7.90–7.93 (m, 2H, Ar-H), 10.43 (s, 1H, SO_2N**H**); Anal. Calcd. for $C_{21}H_{21}N_3O_5S$ (427.47): C, 59.00; H, 4.95; N, 9.83; Found: C, 59.39; H, 4.68; N, 9.49.

4.1.1.10. N-[4-(phthalimdomethyl)phenylsulfonamide]-N'-butylurea **6_d**. White powder (yield 68%); m.p. 128–130 °C; ^{1}H NMR (DMSO-d_6, 600 MHz) δ (ppm): 0.78–0.80 (t, 3H, CH_3), 1.13–1.18 (septet, 2H, CH_2), 1.25–1.30 (p, 2H, CH_2), 2.91–2.94 (q, 2H, CH_2), 4.88 (s, 2H, CH_2), 6.47 (s, 1H, N**H**-CH_2, D_2O exchangeable), 7.53–7.55 (d, 2H, J = 8.4 Hz, Ar-H), 7.85–7.86 (d, 2H, J = 8.4 Hz, Ar-H), 7.87–7.89 (m, 2H, Ar-H),

Table 9
Predicted ADMET for the designed compounds and reference drugs.

Comp.	BBB level[a]	Absorption level[b]	Hepatotoxicity probability[c]	CYP2D6[d]	CYP2D6 probability	PPB[e]	Solubility[f]
5	4	2	0.32	0	0.25	1	2
6_a	4	2	0.44	1	0.75	1	2
6_b	4	2	0.83	1	0.68	1	2
6_c	4	2	0.54	0	0.28	1	2
6_d	4	2	0.77	0	0.50	1	2
6_e	4	2	0.36	0	0.19	1	2
6_f	4	2	0.70	0	0.32	1	2
6_g	4	1	0.42	1	0.58	1	2
6_h	4	1	0.58	1	0.58	1	2
6_i	4	2	0.84	1	0.56	1	2
6_j	4	2	0.51	0	0.24	1	2
6_k	4	2	0.47	0	0.25	1	2
6_l	4	2	0.86	0	0.44	1	2
6_m	4	2	0.34	0	0.24	1	2
6_n	4	2	0.75	0	0.24	1	2
Rosiglitazone	1	0	0.642	0	0.405	1	2
Glibenclamide	4	1	0.231	0	0.326	1	2

[a] BBB level, blood brain barrier level, 0 = very high, 1 = high, 2 = medium, 3 = low, 4 = very low.
[b] Absorption level, 0 = good, 1 = moderate, 2 = poor, 3 = very poor.
[c] Hepatotoxicity probability, value > 0.5 means toxic, value < 0.5 means non-toxic.
[d] CYP2D6, cytochrome P2D6, 0 = non inhibitor, 1 = inhibitor.
[e] PBB, plasma protein binding, 0 means < 90%, 1 means > 90%, 2 means > 95%.
[f] Solubility level, 1 = very low, 2 = low, 3 = good, 4 = optimal.

7.91–7.94 (m, 2H, Ar-H), 10.32–10.71 (br, s, NH); Anal. Calcd. for $C_{20}H_{21}N_3O_5S$ (415.46): C, 57.82; H, 5.10; N, 10.11; Found: C, 57.51; H, 5.52; N, 10.49.

4.1.1.11. N-[4-(phthalimdoethyl)phenylsulfonamide]-N'-cylcopentylurea **6_e**. White crystals (yield 73%); m.p. 198–199 °C; ^{1}H NMR (DMSO-d_6, 600 MHz) δ (ppm): 1.22–1.27 (m, 2H, CH_2), 1.41–1.48 (m, 2H, CH_2), 1.53–1.58 (m, 2H, CH_2), 1.68–1.73 (m, 2H, CH_2), 3.00–3.03 (t, 2H, CH_2), 3.69–3.73(m, 1H, *N*-C**H**), 3.84–4.86 (t, 2H, N-C**H**$_2$), 6.45 (br s, 1H, N**H**-CH_2, D_2O exchangeable), 7.44–7.45 (d, 2H, *J* = 7.8 Hz, Ar-H), 7.77–7.78 (d, 2H, *J* = 7.8 Hz, Ar-H), 7.82–7.85 (m, 4H, Ar-H), 10.35 (s, 1H, SO_2N**H**);; Anal. Calcd. for $C_{22}H_{23}N_3O_5S$ (441.50): C, 59.85; H, 5.25; N, 9.52; Found: C, 59.45; H, 5.66; N, 9.19.

4.1.1.12. N-[4-(phthalimdoethyl)phenylsulfonamide]-N'-butylurea **6_f**. White powder (yield 71%); m.p. 180–182 °C; IR (KBr, υ cm^{-1}): 3422, 3322 (2NH), 2945 (C—H aliphatic), 1680 (C═O); ^{1}H NMR (DMSO-d_6, 600 MHz) δ (ppm): 0.80–0.82 (t, 3H, CH_3), 1.13–1.19 (m, 2H, CH_2), 1.26–1.31 (p, 2H, CH_2), 2.91–2.94 (q, 2H, CH_2), 3.01–3.04 (t, 2H, CH_2), 3.85–3.87 (t, 2H, CH_2), 6.47 (br s,1H, N**H**-CH_2, D_2O exchangeable), 7.44–7.45 (d, 2H, *J* = 8.4 Hz, Ar-H), 7.79–8.00 (d, 2H, *J* = 8.5 Hz, Ar-H), 7.83–7.86 (m, 4H, Ar-H), 10.53 (br s,1H, SO_2N**H**); Anal. Calcd. for $C_{21}H_{23}N_3O_5S$ (429.49): C, 58.73; H, 5.40; N, 9.78; Found: C, 58.43; H, 5.05; N, 9.41.

4.1.1.13. N-[4-(5-Chlorophthalimdo)phenylsulfonyl]-N'-cylcohexylurea **6_g**. White crystals (yield 65%); m.p. 170–172 °C; IR (KBr, υ cm^{-1}): 3328, 3132 (2NH), 3038 (C—H aromatic), 2928 (C—H aliphatic), 1624 (C═O); ^{1}H NMR (DMSO-d_6, 600 MHz) δ (ppm): 1.14–1.24 (m, 3H, CH & CH_2), 1.48–1.50 (m, 2H, CH_2), 1.58–1.61 (m, 3H, CH & CH_2), 1.66–1.68 (br, 2H, CH_2), 3.41 (m, 1H, *N*-CH), 6.43 (s, 1H, N**H**-CH_2, D_2O exchangeable), 7.70–7.72 (d, 2H, ***J*** = 8.4 Hz, Ar-H), 7.92–8.04 (m, 3H, Ar-H), 8.04–8.05 (d, 2H, *J* = 8.4 Hz, Ar-H), 10.50 (s, 1H, N**H**, D_2O exchangeable); Anal. Calcd. for $C_{21}H_{20}ClN_3O_5S$ (461.92): C, 54.49; H, 4.57; N, 9.08; Found: C, 54.40; H, 4.11; N, 9.43.

4.1.1.14. N-[4-(5-Chlorophthalimdo)phenylsulfonyl]-N'-cylcopentylurea **6_h**. White crystals (yield 68%); m.p. 168–169 °C; IR (KBr, υ cm^{-1}): 3347 (2NH), 2937 (C—H aliphatic), 1696 (C═O); ^{1}H NMR (DMSO-d_6, 600 MHz) δ (ppm): 1.24–1.29 (m, 2H, CH_2), 1.41–1.47 (m, 2H, CH_2), 1.51–1.57 (m, 2H, CH_2), 1.69–1.75 (m, 2H, CH_2), 3.72–3.74 (m,1H, *N*-C**H**), 6.68 (s, 1H, N**H**-CH_2), 7.68–7.69 (dd, 2H, *J* = 8.4 Hz, Ar-H), 7.89–7.99 (m, 3H, Ar-H), 8.01–8.03 (dd, 2H, *J* = 8.4 Hz, Ar-H), 10.50 (s, 1H, NH, D_2O exchangeable); Anal. Calcd. for $C_{20}H_{18}ClN_3O_5S$ (447.89): C, 53.63; H, 4.05; N, 9.38; Found: C, 53.26; H, 4.33; N, 9.78.

4.1.1.15. N-[4-(5-Chlorophthalimdo)phenylsulfonyl]-N'-butylurea **6_i**. White powder (yield 73%); m.p. 216–218 °C; ^{1}H NMR (DMSO-d_6, 600 MHz) δ (ppm): 0.76–0.81 (t, 3H, CH_3)1.14–1.18 (m, 2H, CH_2), 1.27–1.31 (m, 2H, CH_2), 2.91–2.94 (q, 2H, CH_2), 6.52 (br s, 1H, N**H**-CH_2, D_2O exchangeable), 7.68–7.70 (dd, 2H, *J* = 8.4 Hz, Ar-H), 7.90–7.99 (m, 3H, Ar-H), 8.00–8.02 (dd, 2H, *J* = 8.4 Hz, Ar-H), 10.50 (s, 1H, NH, D_2O exchangeable); Anal. Calcd. for $C_{19}H_{18}ClN_3O_5S$ (435.88): C, 52.36; H, 4.16; N, 9.64; Found: C, 52.91; H, 4.55; N, 9.34.

4.1.1.16. N-[4-(5-Chlorophthalimdomethyl)phenylsulfonyl]-N'-cylcohexylurea **6_j**. White crystals (yield 70%); m.p. 168–169 °C; IR (KBr, υ cm^{-1}): 3283, 3130 (2NH, overlapped), 3080 (C—H aromatic), 1655 (C═O); ^{1}H NMR (DMSO-d_6, 600 MHz) δ (ppm): 1.01–1.07 (m, 3H, CH & CH_2), 1.12–1.16 (m, 2H, CH_2), 1.43–1.45 (d, 1H, CH), 1.52–1.54 (m, 1H, CH_2), 1.58–1.60 (d, 2H, CH_2), 3.21–3.22 (m, 1H, *N*-CH), 4.83 (s, 2H, CH_2), 6.29 (s, 1H, N**H**-CH_2, D_2O exchangeable), 7.48–7.49 (d, 2H, *J* = 8.4 Hz, Ar-H), 7.80–7.81 (d, 2H, *J* = 8.4 Hz, Ar-H), 7.84–7.89 (m, 3H, Ar-H), 10.48 (s, 1H, SO_2N**H**); Anal. Calcd. for $C_{22}H_{22}ClN_3O_5S$ (475.95): C, 55.52; H, 4.66; N, 8.83; Found: C, 55.11; H, 4.23; N, 8.48.

4.1.1.17. N-[4-(5-Chlorophthalimdomethyl)phenylsulfonyl]-N'-cylcopentylurea **6_k**. White crystals (yield 59%); m.p. 161–163 °C; IR (KBr, υ cm^{-1}): 3348 (2NH), 2937 (C—H aliphatic), 1695 (C═O); ^{1}H NMR (DMSO-d_6, 600 MHz) δ (ppm): 1.19–1.24 (m, 2H, CH_2), 1.37–1.39 (m, 2H, CH_2), 1.50–1.51 (m, 2H, CH_2), 1.65–1.69 (m, 2H, CH_2), 3.67–3.78 (m,1H, *N*-C**H**), 4.82 (s, 2H, CH_2), 6.42 (br, s 1H, N**H**-CH_2, D_2O exchangeable), 7.48–7.50 (d, 2H, *J* = 8.4 Hz, Ar-H), 7.80–7.82 (d, 2H, *J* = 8.4 Hz, Ar-H), 7.82–7.91 (m, 3H, Ar-H), 10.50 (s, 1H, SO_2N**H**); Anal. Calcd. for $C_{21}H_{20}ClN_3O_5S$ (461.92): C, 54.61; H, 4.36; N, 9.10; Found: C, 54.28; H, 4.88; N, 9.51.

4.1.1.18. N-[4-(5-Chlorophthalimdomethyl)phenylsulfonyl]-N'-butylurea **6_l**. White powder (yield 64%); m.p. 174–175 °C; IR (KBr, υ cm^{-1}): 3241 (2NH, overlapped), 2944 (C—H aliphatic), 1689 (C═O); ^{1}H NMR

(DMSO-d_6, 600 MHz) δ (ppm): 0.73–0.75 (t, 3H, CH_3)1.06–1.13 (m, 2H, CH_2), 1.19–1.25 (m, 2H, CH_2), 2.86–2.90 (q, 2H, CH_2), 4.83 (s, 2H, CH_2), 6.43 (br s, 1H, N**H**-CH_2, D_2O exchangeable), 7.49–7.50 (d, 2H, J = 8.4 Hz, Ar-H), 7.81–7.82 (d, 2H, J = 8.4 Hz, Ar-H), 7.83–7.92 (m, 3H, Ar-H), 10.51 (s, 1H, SO_2N**H**); Anal. Calcd. for $C_{20}H_{20}ClN_3O_5S$ (449.91): C, 53.39; H, 4.48; N, 9.34; Found: C, 53.01; H, 4.09; N, 9.80.

4.1.1.19. N-[4-(5-Chlorophthalimdoethyl)phenylsulfonyl]-N'-cylcopentylurea 6_m. White crystals (yield 67%); m.p. 114–116 °C; IR (KBr, υ cm^{-1}): 3345 (2NH, overlapped), 3074 (C—H aromatic), 2934 (C—H aliphatic), 1694 (C═O); ^{1}H NMR (DMSO-d_6, 600 MHz) δ (ppm): 1.19–1.22 (m, 2H, CH_2), 1.41–1.43 (m, 2H, CH_2), 1.50–1.51 (m, 2H, CH_2), 1.65–1.68 (m, 2H, CH_2), 2.99–3.01 (m, 2H, CH_2), 3.66–3.69 (m, 2H, CH_2), 3.98–4.11 (m, 2H, N-CH_2), 6.41 (s, 1H, NH, D_2O exchangeable), 7.66–7.67 (d, 2H, J = 8.4 Hz, Ar-H), 7.72–7.73 (d, 2H, J = 8.4 Hz, Ar-H), 7.79–7.81 (m, 3H, Ar-H), 10.47 (s, 1H, SO_2N**H**); Anal. Calcd. for $C_{22}H_{22}ClN_3O_5S$ (475.95): C, 56.15; H, 5.33; N, 8.54; Found: C, 56.51; H, 5.89; N, 8.12.

4.1.1.20. N-[4-(5-Chlorophthalimdoethyl)phenylsulfonyl]-N'-butylurea 6_n. White powder (yield 68%); m.p. 162–164 °C; IR (KBr, υ cm^{-1}): 3377, 3300 (2NH, overlapped), 3052 (C—H aromatic), 1698 (C═O); ^{1}H NMR (DMSO-d_6, 600 MHz) δ (ppm): 0.74–0.76 (t, 3H, CH_3), 1.08–1.12 (m, 2H, CH_2), 1.21–1.25 (m, 2H, CH_2), 2.86–2.89 (q, 2H, CH_2), 2.98–3.00 (m, 2H, CH_2), 3.82–3.85 (m, 2H, CH_2), 6.45 (s, 1H, N**H**-CH_2, D_2O exchangeable), 7.38–7.39 (d, 2H, J = 8.4 Hz, Ar-H), 7.72–7.73 (d, 2H, J = 8.4 Hz, Ar-H), 7.80–7.84 (m, 3H, Ar-H), 10.50 (s, 1H, SO_2N**H**); Anal. Calcd. for $C_{21}H_{22}ClN_3O_5S$ (463.93): C, 54.37; H, 4.78; N, 9.06; Found: C, 54.80; H, 4.41; N, 9.47.

4.2. Biology

4.2.1. Animals

Male Wistar Albino rats 5–7 months and weight range of 200–250 g, were purchased from the animal house of King Fahed Medical Research Center King Abdulaziz University. Animals were housed under conventional conditions and were allowed free access with standard diet and water. They were kept in clean and dry cages and maintained in well-ventilated animal house with 12 h light-12 h dark cycle.

4.2.2. Induction of experimental diabetes

A freshly prepared solution of streptozotocin (STZ) dissolved in 0.1 M sodium citrate buffer (pH 4.5) just before use and injected intraperitoneally in a dose of 55 mg/kg body weight to overnight fastening rats [36]. Control animals (n = 6) received an equivalent volume of citrate buffer. Ten days after STZ administration, the diabetic rats with blood glucose concentration between 20 and 30 mmol /L (360 – 540 mg/dL) were selected for the experimental protocol deigned below. The samples were analyzed for blood glucose content by using One Touch Ultra (Lifescan, A Gohnson& Gohnson Company).

4.2.3. In vivo anti-hyperglycemic activity

The synthesized compounds and reference drug (glibinclamide) were suspended in 5% CMC. Ninety diabetic rats were arranged into 15 groups (n = 6), one diabetic group received CMC as a solvent and served as a negative control. Another group were treated with glibinclamide (5.00 mg/kg) as a reference standard. The other thirteen groups were administered the synthesized compounds orally in a dose of 5.00 mg/kg. Blood samples were withdrawn from the tail tip and blood glucose levels were determined two hours later for 7 days. Blood glucose levels were measured immediately by One Touch Ultra (Lifescan, A Gohnson & Gohnson Company). The median of % reduction in blood glucose levels was calculated.

4.2.4. Oral glucose Tolerance test (OGTT)

After two hours of solvent, glibinclamide and the tested compounds were administered for the control and the diabetic-treated groups, the rats of normal and diabetic groups were orally treated with 2 g/kg of glucose. Blood samples (one drop) were collected from the tail vein at 0.0, 30, 60, 90 and 120 min after glucose loading. Blood glucose was determined at these time intervals using One Touch Ultra. The area under the curve (AUC) was calculated by the trapezoidal method. The AUCs of the curves of each group were compared and tested for significance from the control groups, to represent the glucose utilization by tissues. Data are expressed as mean ± standard error of mean. The significance of differences between the control and the test groups was established using the Student's *t*-test for paired data. Significance was set at $p < 0.05$ [37].

4.3. Molecular modeling

4.3.1. Docking studies

Crystallographic structure of PPARγ was retrieved from Protein Data Bank [PDB ID- 1FM6, resolution 2.1 Å] (http://www.pdb.org), and considered as a target for docking simulations. The docking analysis was performed using MOE [45] software to evaluate the free energies and binding mode of the designed molecules against PPARγ. At first, the crystal structure of PPARγ was prepared by removing water molecules and retaining only one chain and its co-crystallized ligand, rosiglitasone. Then, the protein structure was protonated, and the hydrogen atoms were hided. Next, the energy was minimized, and the binding pocket of the protein was defined.

The 2D structures of the synthesized compounds, rosiglitazone and glibenclamide were sketched using ChemBioDraw Ultra 14.0 and saved as MDL-SD format. Then, the saved file was opened using MOE and 3D structures were protonated. Next, energy minimization was applied. Before docking the synthesized compounds, validation of the docking protocol was carried out by running the simulation only using the co-crystallized ligand and low RMSD between docked and crystal conformations. The molecular docking of the synthesized compounds and reference ligands (rosiglitazone and glibenclamide) was performed using a default protocol. In each case, 30 docked structures were generated using genetic algorithm searches. The output from of MOE was further analyzed with Discovery Studio 2.5 software.

4.3.2. Pharmacophore studies

Pharmacophore model for SUR agonists was carried out using Discovery Studio 2.5 software. A data set of thirty one sulfonylurea containing compounds with diverse structures and variable activities were selected from the literature [25,26,46] **(**Fig. 15**)**. Twenty compounds were used as a training set and eleven compounds were used as a test set. The training set was used for generation of pharmacophore model, where the test set was utilized to validate the generated pharmacophore hypothesis. Glibenclamide, was used as the reference SU agonist. The selected compounds were prepared for pharmacophore generation via prepare ligand protocol. 3D QSAR Pharmacophore generation protocol was used for building pharmacophore model. In this protocol, we used the following features in pharmacophore generation; i) hydrogen bond donor (HBD), ii) hydrogen bond acceptor (HBA), iii) hydrophobic aliphatic (HA), iii) hydrophobic aromatic (HAr), and ring aromatic (RA). Then, ligand pharmacophore mapping protocol was used in virtual screening process. The most predictive model was used as 3D queries to identify potential leads against SUR from the newly synthesized compounds

4.3.3. QSAR studies

The previously generated and validated QSAR models [26] were used for predicting the PPARγ binding affinity (IC_{50}) and insulin-secreting ability (EC_{50}) of the synthesized compounds. Discovery studio 2.5 software was used for performing this studies.

Calculate molecular properties protocol was used to calculate the predicted pIC_{50} (−log IC50) and pEC_{50} (−log EC50) depending on the

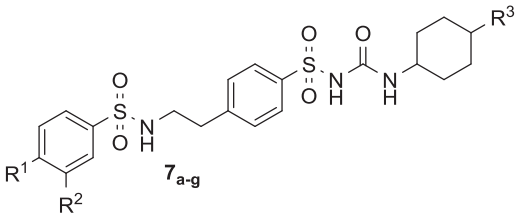

a)[x] R^1= Br, R^2 = H, R^3= CH_3
b)[x] R^1= H, R^2 = H, R^3= H
c)[x] R^1= H, R^2 = H, R^3= CH_3
d)[x] R^1= Cl, R^2 = H, R^3= H
e)[x] R^1= Br, R^2 = H, R^3= H
f)[y] R^1= $NHCOCH_3$, R^2 = H, R^3= CH_3
g)[y] R^1= $NHCOCH_3$, R^2 = CH_3, R^3= CH_3

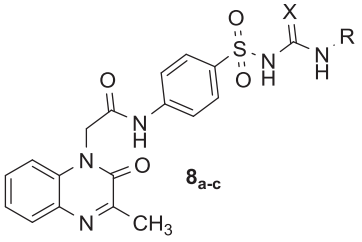

a)[x] R= Cyclohexyl, X = O
b)[x] R= Butyl , X = O
c)[y] R= Phenyl, X = O

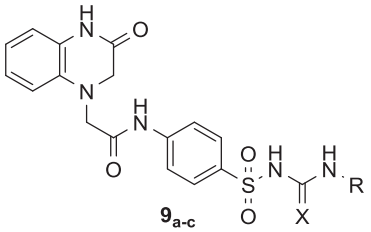

a)[x] R= Cyclohexyl, X = O
b)[x] R= Butyl , X = O
c)[y] R= Phenyl, X = O

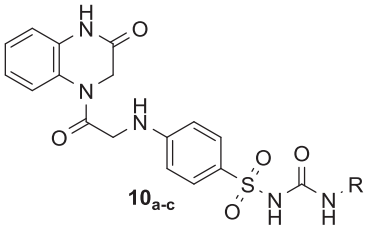

a)[x] R= Cyclohexyl,
b)[x] R= Butyl
c)[y] R= Phenyl

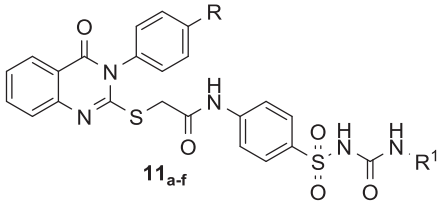

a)[x] R = CH_3, R^1= Cyclohexyl
b)[x] R = CH_3, R^1= Phenyl
c)[x] R = CH_3, R^1= Butyl
d)[x] R^1= OCH_3, R= Cyclohexyl
e)[y] R^1= OCH_3, R= Phenyl
f)[y] R^1= OCH_3, R= Butyl

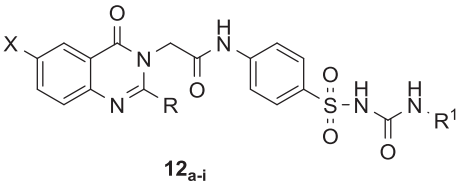

a)[x] X = H, R = CH_3, R^1= Cyclohexyl
b)[x] X = H, R = CH_3, R^1= Phenyl
c)[x] X = H, R = CH_3, R^1= Butyl
d)[x] X = H, R = CH_2CH_3, R^1= Cyclohexyl
e)[x] X = H, R = CH_2CH_3, R^1= Phenyl
f)[y] X = H, R = CH_2CH_3, R^1= Butyl
g)[y] X = Br, R = CH_3, R^1= Cyclohexyl
h)[y] X = Br, R = CH_3, R^1= Phenyl
i)[y] X = Br, R = CH_3, R^1= Butyl

[x] Training set: Compounds $\mathbf{7_{a-e}}$, $\mathbf{8_{a,b}}$, $\mathbf{9_{a,b}}$, $\mathbf{10_{d,b}}$, $\mathbf{11_{a-d}}$, $\mathbf{12_{a-e}}$

[y] Test set: Compounds $\mathbf{7_{f,g}}$, $\mathbf{8_c}$, $\mathbf{9_c}$, $\mathbf{10_c}$, $\mathbf{11_{e,f}}$, $\mathbf{12_{f-i}}$

Fig. 15. Chemical structures of training set and test set molecules. [x]Training set: Compounds $\mathbf{7_{a-e}}$, $\mathbf{8_{a,b}}$, $\mathbf{9_{a,b}}$, $\mathbf{10_{d,b}}$, $\mathbf{11_{a-d}}$, $\mathbf{12_{a-e}}$. [y]Test set: Compounds $\mathbf{7_{f,g}}$, $\mathbf{8_c}$, $\mathbf{9_c}$, $\mathbf{10_c}$, $\mathbf{11_{e,f}}$, $\mathbf{12_{f-i}}$.

generated QSAR models. The predicted IC_{50} and EC_{50} were calculated from the equations of 10^{-pIC50} and 10^{-pEC50}, respectively.

4.3.4. In silico ADMET analysis

Absorption, distribution, metabolism, excretion and toxicity (ADMET) prediction was carried out with the ADMET descriptor module of the small molecules protocol of Discovery studio 2.5 software.

Acknowledgements

This research is supported by The Research and Consultations Institute of King Abdulaziz University, Project No. (428 / 044).

References

[1] E. Sithole, World facing diabetes catastrophe: Experts, Reuters Health Report, Paris, 25, 2003.

[2] G. Bruno, B. Lorenzati, C. Zucco, S. Miglietta, F. Lamberti, Oral hypoglycemic drugs &58; pathophysiological basis of their mechanism of actionoral hypoglycemic drugs &58; pathophysiological basis of their mechanism of action, Pharmaceuticals 3 (2010) 3005–3020.

[3] U. Panten, M. Schwanstecher, C. Schwanstecher, Sulfonylurea receptors and mechanism of sulfonylurea action, Exp. Clin. Endocrinol. Diabetes 104 (1996) 1–9.

[4] M. Ricote, A.C. Li, T.M. Willson, C.J. Kelly, C.K. Glass, The peroxisome proliferator-activated receptor-γ is a negative regulator of macrophage activation, Nature 391 (1998) 79–82.

[5] C.J. Bailey, R.C. Turner, Metformin, N. Engl. J. Med. 334 (1996) 574–579.

[6] F.M. Ashcroft, Mechanisms of the glycaemic effects of sulfonylureas, Horm. Metab. Res. 28 (1996) 456–463.

[7] D.A. Nelson, J. Bryan, S. Wechsler, J.P. Clement IV, L. Aguilar-Bryan, The high-affinity sulfonylurea receptor: distribution, glycosylation, purification, and immunoprecipitation of two forms from endocrine and neuroendocrine cell lines, Biochemistry 35 (1996) 14793–14799.

[8] R. Bressler, D.G. Johnson, Pharmacological regulation of blood glucose levels in non—insulin-department diabetes mellitus, Arch. Intern. Med. 157 (1997) 836–848.

[9] H. Sakura, C. Ämmälä, P. Smith, F. Gribble, F. Ashcroft, Cloning and functional expression of the cDNA encoding a novel ATP-sensitive potassium channel subunit expressed in pancreatic β-cells, brain, heart and skeletal muscle, FEBS Lett. 377 (1995) 338–344.

[10] N. Inagaki, T. Gonoi, J.P. Clement, N. Namba, J. Inazawa, G. Gonzalez, L. Aguilar-Bryan, S. Seino, J. Bryan, Reconstitution of IKATP: an inward rectifier subunit plus the sulfonylurea receptor, Science 270 (1995) 1166–1170.

[11] M. Bodmer, C. Meier, S. Krähenbühl, S.S. Jick, C.R. Meier, Metformin, sulfonylureas, or other antidiabetes drugs and the risk of lactic acidosis or hypoglycemia, Diabetes Care 31 (2008) 2086–2091.

[12] L.C. Groop, Sulfonylureas in NIDDM, Diabetes Care 15 (1992) 737–754.

[13] S. Fukuen, M. Iwaki, A. Yasui, M. Makishima, M. Matsuda, I. Shimomura, Sulfonylurea agents exhibit peroxisome proliferator-activated receptor γ agonistic activity, J. Biol. Chem. 280 (2005) 23653–23659.

[14] A. Arrault, S. Rocchi, F. Picard, P. Maurois, B. Pirotte, J. Vamecq, A short series of antidiabetic sulfonylureas exhibit multiple ligand PPARγ-binding patterns, Biomed. Pharmacother. 63 (2009) 56–62.

[15] C. Kharbanda, M.S. Alam, H. Hamid, K. Javed, A. Dhulap, S. Bano, Y. Ali, Antidiabetic effect of novel benzenesulfonylureas as PPAR-γ agonists and their anticancer effect, Biorg. Med. Chem. Lett. 25 (2015) 4601–4605.

[16] W.H. Vila-Carriles, G. Zhao, J. Bryan, Defining a binding pocket for sulfonylureas in ATP-sensitive potassium channels, FASEB J. 21 (2007) 18–25.

[17] Y. Yang, A.E. Lovett-Racke, M.K. Racke, Regulation of immune responses and autoimmune encephalomyelitis by PPARs, PPAR Res. 2010 (2010).

[18] D.P. Marciano, M.R. Chang, C.A. Corzo, D. Goswami, V.Q. Lam, B.D. Pascal, P.R. Griffin, The therapeutic potential of nuclear receptor modulators for treatment of metabolic disorders: PPARγ, RORs, and Rev-erbs, Cell Metab. 19 (2014) 193–208.

[19] N. Mahindroo, C.-F. Huang, Y.-H. Peng, C.-C. Wang, C.-C. Liao, T.-W. Lien, S.K. Chittimalla, W.-J. Huang, C.-H. Chai, E. Prakash, Novel indole-based peroxisome proliferator-activated receptor agonists: design, SAR, structural biology, and biological activities, J. Med. Chem. 48 (2005) 8194–8208.

[20] B.Y. Kim, J.B. Ahn, H.W. Lee, S.K. Kang, J.H. Lee, J.S. Shin, S.K. Ahn, C.I. Hong, S.S. Yoon, Synthesis and biological activity of novel substituted pyridines and purines containing 2, 4-thiazolidinedione, Eur. J. Med. Chem. 39 (2004) 433–447.

[21] T. Larsen, S. Toubro, A. Astrup, PPARgamma agonists in the treatment of type II diabetes: is increased fatness commensurate with long-term efficacy? Int. J. Obesity 27 (2003) 147–161.

[22] A.-M. Alaa, A.S. El-Azab, S.M. Attia, A.M. Al-Obaid, M.A. Al-Omar, H.I. El-Subbagh, Synthesis and biological evaluation of some novel cyclic-imides as hypoglycaemic, anti-hyperlipidemic agents, Eur. J. Med. Chem. 46 (2011) 4324–4329.

[23] H. Weber, W. Aumuller, R. Weyer, K. Muth, F.H. Schmidt, Benzenesulfonyl-ureas and process for their manufacture, in, Google Patents, 1969.

[24] H. Weber, W. Aumuller, R. Weyer, K. Muth, F.H. Schmidt, Benzenesulfonyl ureas as anti-diabetic agents, in, Google Patents, 1970.

[25] M.K. Ibrahim, I.H. Eissa, A.E. Abdallah, A.M. Metwaly, M. Radwan, M. ElSohly, Design, synthesis, molecular modeling and anti-hyperglycemic evaluation of novel quinoxaline derivatives as potential PPARγ and SUR agonists, Biorg. Med. Chem. 25 (2017) 1496–1513.

[26] M.K. Ibrahim, I.H. Eissa, M.S. Alesawy, A.M. Metwaly, M.M. Radwan, M.A. ElSohly, Design, synthesis, molecular modeling and anti-hyperglycemic evaluation of quinazolin-4 (3H)-one derivatives as potential PPARγ and SUR agonists, Biorg. Med. Chem. 25 (2017) 4723–4744.

[27] I.H. Eissa, H. Mohammad, O.A. Qassem, W. Younis, T.M. Abdelghany, A. Elshafeey, M.M.A.R. Moustafa, M.N. Seleem, A.S. Mayhoub, Diphenylurea derivatives for combating methicillin-and vancomycin-resistant Staphylococcus aureus, Eur. J. Med. Chem. 130 (2017) 73–85.

[28] M. Ibrahim, M. Taghour, A. Metwaly, A. Belal, A. Mehany, M. Elhendawy, M. Radwan, A. Yassin, N. El-Deeb, E. Hafez, Design, synthesis, molecular modeling and anti-proliferative evaluation of novel quinoxaline derivatives as potential DNA intercalators and topoisomerase II inhibitors, Eur. J. Med. Chem. 155 (2018) 117–134.

[29] A.A. Gaber, A.H. Bayoumi, A.M. El-morsy, F.F. Sherbiny, A.B. Mehany, I.H. Eissa, Design, synthesis and anticancer evaluation of 1H-pyrazolo [3, 4-d] pyrimidine derivatives as potent EGFR WT and EGFR T790M inhibitors and apoptosis inducers, Bioorg. Chem. 80 (2018) 375–395.

[30] V. Zoete, A. Grosdidier, O. Michielin, Peroxisome proliferator-activated receptor structures: ligand specificity, molecular switch and interactions with regulators, Biochim. Biophys. Acta (BBA)-Mol. Cell Biol. Lipids 1771 (2007) 915–925.

[31] A. Pharmacodynamics, Clinical Pharmacology of Sulfonylureas, Oral antidiabetics, 1996, 199.

[32] V.A. Dixit, P.V. Bharatam, SAR and computer-aided drug design approaches in the discovery of peroxisome proliferator-activated receptor γ activators: A perspective, J. Comput. Med. 2013 (2013).

[33] J.L. Santos, P.R. Yamasaki, C.M. Chin, C.H. Takashi, F.R. Pavan, C.Q. Leite, Synthesis and in vitro anti Mycobacterium tuberculosis activity of a series of phthalimide derivatives, Biorg. Med. Chem. 17 (2009) 3795–3799.

[34] I.A. Al-Suwaidan, A.M. Alanazi, A.S. El-Azab, A.M. Al-Obaid, K.E. ElTahir, A.R. Maarouf, M.A.A. El-Enin, A.-M. Alaa, Molecular design, synthesis and biological evaluation of cyclic imides bearing benzenesulfonamide fragment as potential COX-2 inhibitors. Part 2, Biorg. Med. Chem. Lett. 23 (2013) 2601–2605.

[35] A.-M. Alaa, A. Angeli, A.S. El-Azab, M.A.A. El-Enin, C.T. Supuran, Synthesis and biological evaluation of cyclic imides incorporating benzenesulfonamide moieties as carbonic anhydrase I, II, IV and IX inhibitors, Biorg. Med. Chem. 25 (2017) 1666–1671.

[36] D.J. Ramsey, H. Ripps, H. Qian, Streptozotocin-induced diabetes modulates GABA receptor activity of rat retinal neurons, Exp. Eye Res. 85 (2007) 413–422.

[37] M. Stumvoll, A. Mitrakou, W. Pimenta, T. Jenssen, H. Yki-Järvinen, T. Van Haeften, W. Renn, J. Gerich, Use of the oral glucose tolerance test to assess insulin release and insulin sensitivity, Diabetes Care 23 (2000) 295–301.

[38] S. Bajare, J. Anthony, A. Nair, R. Marita, A. Damre, D. Patel, C. Rao, H. Sivaramakrishnan, N. Deka, Synthesis of N-(5-chloro-6-(quinolin-3-yloxy) pyridin-3-yl) benzenesulfonamide derivatives as non-TZD peroxisome proliferator-activated receptor γ (PPARγ) agonist, Eur. J. Med. Chem. 58 (2012) 355–360.

[39] A.-G.A. El-Helby, R.R. Ayyad, K. El-Adl, H. Sakr, A.A. Abd-Elrahman, I.H. Eissa, A. Elwan, Design, molecular docking and synthesis of some novel 4-acetyl-1-substituted-3, 4-dihydroquinoxalin-2 (1H)-one derivatives for anticonvulsant evaluation as AMPA-receptor antagonists, Med. Chem. Res. 25 (2016) 3030–3046.

[40] A.M. El-Naggar, M.M. Abou-El-Regal, S.A. El-Metwally, F.F. Sherbiny, I.H. Eissa, Synthesis, characterization and molecular docking studies of thiouracil derivatives as potent thymidylate synthase inhibitors and potential anticancer agents, Mol. Diversity (2017) 1–17.

[41] W.M. Eldehna, M.F. Abo-Ashour, A. Nocentini, P. Gratteri, I.H. Eissa, M. Fares, O.E. Ismael, H.A. Ghabbour, M.M. Elaasser, H.A. Abdel-Aziz, Novel 4/3-((4-oxo-5-(2-oxoindolin-3-ylidene) thiazolidin-2-ylidene) amino) benzenesulfonamides: Synthesis, carbonic anhydrase inhibitory activity, anticancer activity and molecular modelling studies, Eur. J. Med. Chem. 139 (2017) 250–262.

[42] I.H. Eissa, A.M. El-Naggar, M.A. El-Hashash, Design, synthesis, molecular modeling and biological evaluation of novel 1H-pyrazolo [3, 4-b] pyridine derivatives as potential anticancer agents, Bioorg. Chem. 67 (2016) 43–56.

[43] H. Li, J.-P. Wang, F. Yang, Design, synthesis and biological activity evaluation of 2-mercapto-4 (3H)-quinazolinone derivatives as novel inhibitors of protein tyrosine phosphatase 1B, Heterocycles: An Int. J. Rev. Commun. Heterocycl. Chem. 85 (2012) 1897–1911.

[44] A.G.A. El-Helby, R.R. Ayyad, H.M. Sakr, A.S. Abdelrahim, K. El-Adl, F.S. Sherbiny, I.H. Eissa, M.M. Khalifa, Design, synthesis, molecular modeling and biological evaluation of novel 2, 3-dihydrophthalazine-1, 4-dione derivatives as potential anticonvulsant agents, J. Mol. Struct. 1130 (2017) 333–351.

[45] Chemical Computing Group, Molecular Operating Environment (MOE), http://www.chemcomp.com/ (Accessed in May 2017), in.

[46] H.-B. Zhang, Y.-A. Zhang, G.-Z. Wu, J.-P. Zhou, W.-L. Huang, X.-W. Hu, Synthesis and biological evaluation of sulfonylurea and thiourea derivatives substituted with benzenesulfonamide groups as potential hypoglycemic agents, Bioorg. Med. Chem. Lett. 19 (2009) 1740–1744.

[47] I. Eissa, A. El-Naggar, N. El-Sattar, A. Youssef, Design and discovery of novel quinoxaline derivatives as dual DNA intercalators and topoisomerase II inhibitors, Anti-Cancer Agents Med. Chem. 18 (2) (2018) 195–209.

[48] K.M. El-Gamal, A.M. El-Morsy, A.M. Saad, I.H. Eissa, M. Alswah, Synthesis, docking, QSAR, ADMET and antimicrobial evaluation of new quinoline-3-carbonitrile derivatives as potential DNA-gyrase inhibitors, J. Mol. Struct. 1166 (2018) 15–33.

[49] H. Patel, K. Dhangar, Y. Sonawane, S. Surana, R. Karpoormath, N. Thapliyal, M. Shaikh, M. Noolvi, R. Jagtap, In search of selective 11β-HSD type 1 inhibitors without nephrotoxicity: An approach to resolve the metabolic syndrome by virtual based screening, Arabian J. Chem. 11 (2) (2015) 221–232.